

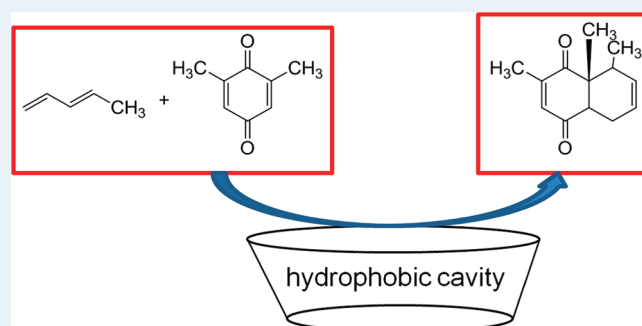
Biomimetic Catalysis

Louis Marchetti and Mindy Levine*

Department of Chemistry, University of Rhode Island, 51 Lower College Road, Kingston, Rhode Island 02881, United States

ABSTRACT: The field of biomimetic chemistry encompasses a wide variety of subfields, including biomimetic catalysis, bio-inspired self-assembly, and biomimetic reactions in total synthesis. Reviewed herein are select examples of biomimetic catalysis using macrocycles and polymeric catalysts. Such catalysts have been used in a variety of synthetic reactions, including several examples of Diels–Alder cycloadditions. Moreover, biomimetic catalysis has influenced the development of the highly active research area of organocatalysis. Several examples of the connections between biomimetic catalysis and organocatalysis are also discussed.

KEYWORDS: biomimetic, catalysis, cyclodextrin, polyethyleneimine, hydrophobic effect



I. INTRODUCTION

“Biomimetic chemistry” is a term that was first used in 1972^{1–4} to describe chemistry that is inspired by biological processes. Biomimetic chemistry covers a wide array of topics that include the synthesis and study of artificial enzymes,⁵ the self-assembly of small molecules in a manner similar to that of biological self-assembly,⁶ and the study of biological precedents to direct the total synthesis of natural products.⁷ In the field of biomimetic chemistry, researchers attempt to utilize the key principles and concepts used in biological systems for the purpose of developing new chemical reactions and processes. “Biomimetic catalysis” generally refers to chemical catalysis that mimics certain key features of enzymatic systems. In this review, we will focus primarily on catalysis using organic macrocycles and polymers. These molecules, like enzymes, create a supramolecular environment that differs from the environment of the bulk medium. In particular, this review covers the following classes of catalysts: cyclodextrin,⁵ cucurbituril, metal-directed macrocycles, synthetic cavitands, polyethyleneimine,^{8,9} and molecularly imprinted polymers. The relationship of biomimetic catalysis to the newer research area of organocatalysis is discussed near the end of this review. There are many other types of biomimetic catalysis, including biomimetic electrocatalysis¹⁰ and biomimetic inorganic catalysis,¹¹ which are not discussed herein. For a more comprehensive discussion, readers are directed toward several excellent reviews.^{12,13}

In constructing artificial enzyme mimics, researchers have focused on several features of enzymes that facilitate efficient catalysis,^{14–16} including (1) high enzyme–substrate binding affinities, (2) high catalytic turnovers of enzyme-catalyzed reactions, and (3) substantial rate accelerations relative to uncatalyzed reactions. Each of these features is discussed in turn.

(1) High enzyme–substrate binding affinities result from the optimized active site of the enzyme, which is complementary in shape and charge distribution to the target substrate. The active

site often contains catalytically active amino acids that assist in reaction catalysis. For example, serine, aspartate, and histidine (the “catalytic triad” of amino acids) are typically found in the active site of proteases and are intimately involved in catalysis.¹⁷ Reactions catalyzed by such enzymes proceed nine orders of magnitude faster than the uncatalyzed reactions.¹⁸

High enzyme–substrate binding affinities also result from hydrophobic binding of the substrate in the enzymatic active site. Hydrophobic binding refers to the favorable interaction of two hydrophobic species in a polar aqueous environment.¹⁹ The hydrophobic molecules are attracted to each other due to their mutual phobia of water. The favorable binding arises from complementary van der Waals attraction²⁰ as well as the desire for water molecules to maximize the number of hydrogen bonds by excluding nonpolar substrates. The active sites of enzymes are usually hydrophobic, which enables hydrophobic substrates to bind in the interiors.²¹

Enzymatic reactions that take place in a hydrophobic environment generally occur faster than they would in water. This rate acceleration can be attributed to the fact that many enzymatic mechanisms are catalyzed by general acids and bases. These reagents are solvated by water molecules in an aqueous medium and need to undergo desolvation to react with the substrate. Reactions that occur in the hydrophobic pocket require less desolvation to proceed. Many enzyme mimics discussed herein rely on hydrophobic binding to bind the substrate efficiently.

(2) High catalytic turnover is a key feature of enzymatic catalysis. It occurs because enzymes have the highest affinity for the reaction transition state, rather than the reactants or products.²² This stabilizes the transition state and lowers the

Special Issue: Biocatalysis and Biomimetic Catalysis for Sustainability

Received: March 31, 2011

Revised: July 12, 2011

Published: August 04, 2011

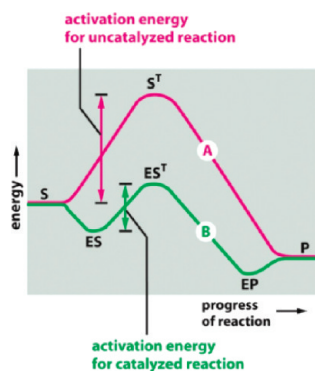


Figure 1. Reaction coordinate for an enzyme-catalyzed reaction.

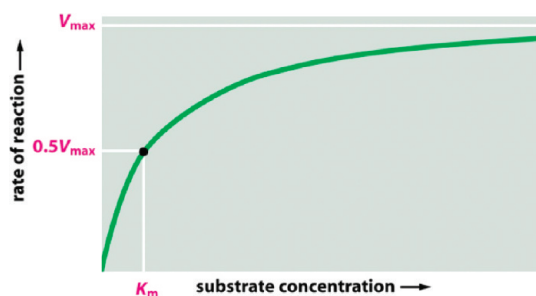


Figure 2. Michaelis–Menten model of enzyme kinetic behavior.

activation energy for the entire reaction (Figure 1). Moreover, high product concentrations generally do not lead to enzymatic inhibition, which enables high catalytic turnover. Synthetic enzymes, such as molecularly imprinted polymers, imitate the high affinity of enzymes for the transition state by using a small-molecule transition state mimic to template the artificial enzymatic active site.

(3) Substantial rate accelerations can be achieved by enzymes. For example, the decarboxylation of orotic acid proceeds 10^{17} times faster in the presence of the enzyme orotidine 5'-phosphate decarboxylase compared with its reaction in neutral aqueous solution.²³ The high rate accelerations can be attributed to both high substrate binding affinities and high catalytic turnovers.

The kinetic behavior of enzymes can often be described by Michaelis–Menten kinetics.²⁴ In this model, the enzyme and substrate reversibly form an enzyme–substrate complex in a pre-equilibrium step. The rate-determining step is the conversion of the bound substrate to product. One consequence of this model is that the reaction rate approaches saturation at high substrate concentrations (Figure 2). Many artificial enzyme mimics discussed herein exhibit Michaelis–Menten kinetic behavior.

The field of biomimetic catalysis has led to the development of a number of highly efficient and selective new catalysts. Research in this field has also led indirectly to the development of organocatalysis, which is an active research area that has achieved tremendous success. The development of organocatalysis, as well as some notable achievements in this field, is discussed in detail later in this review article.

II. CYCLODEXTRINS

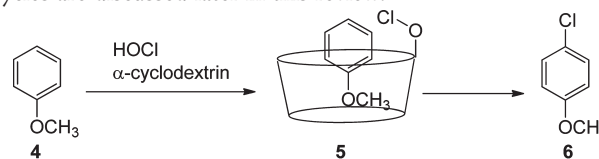
Ila. Introduction. Cyclodextrins are a class of cyclic oligosaccharides composed of glucose monomers. The most commonly used

and commercially available isomers are shown in Figure 3.²⁵ Cyclodextrins have been studied extensively as biomimetic catalysts,^{26–29} and several excellent reviews have been published.^{5,30–36}

The popularity of cyclodextrins can be traced to a number of factors:

- (1) their widespread availability, especially of the isomers shown in Figure 3;
- (2) well-established synthetic methods to modify the hydroxyl groups,^{37,38} which allow a variety of substituents to be introduced;³⁹ and
- (3) the hydrophobic cavity of cyclodextrin, which enables the binding of hydrophobic guests.^{40,41}

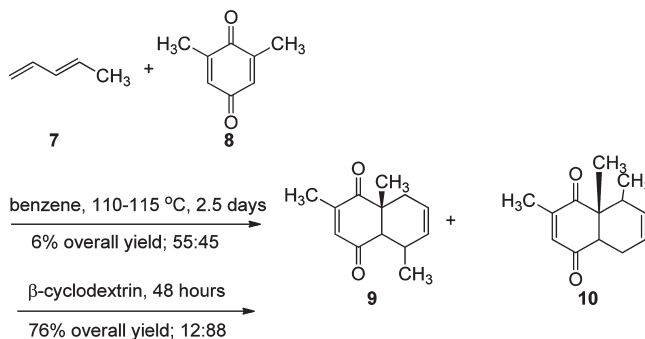
The binding geometry of cyclodextrin to small-molecule guests is generally flexible and somewhat unpredictable, in contrast to other cage compounds (i.e., cucurbituril^{42–44} and synthetic cavitands^{45,46}) that display more rigid binding. These macrocycles are discussed later in this review.



Equation 1: Regiospecific para-chlorination of anisole **4** in an cyclodextrin complex (reprinted from Ref. 47)

Ilb. Catalysis. One early reaction that involved cyclodextrin was the chlorination of anisole complexed in α -cyclodextrin (eq 1),^{47–49} although other examples were reported previously.^{50–52} In this case, cyclodextrin acts as a microreactor to direct the regioselectivity of chlorination, rather than a true catalyst. The para-chlorinated compound **6** is the only product observed. It results from cyclodextrin binding anisole in a well-defined geometry. In contrast, both the non-catalyzed reaction and the enzyme-catalyzed reaction⁵³ produce a mixture of ortho- and para-chlorinated products.

Other instances of the use of cyclodextrin have since been reported.^{54,55} For instance, β -cyclodextrin catalyzes the Diels–Alder reaction of acrylonitrile and cyclopentadiene.^{40,56} The Diels–Alder reaction of 1-methyl butadiene **7** and 2,6-dimethyl-*p*-benzoquinone **8** occurs substantially faster in the presence of an equimolar amount of β -cyclodextrin (eq 2), although again, the cyclodextrin is not acting as a “true” catalyst.⁵⁷ The reaction in the presence of β -cyclodextrin is highly regioselective because cyclodextrin binds the reactants in a well-defined geometry.



Equation 2: Cyclodextrin-promoted Diels–Alder reaction of 1-methyl butadiene **7** with dimethyl benzoquinone **8** (reprinted from Ref. 57)

Another reaction that is accelerated in the presence of β -cyclodextrin is the synthesis of quinoxaline **13** from phenacyl bromide **11** and benzene-1,2-diamine **12** (eq 3).²⁸

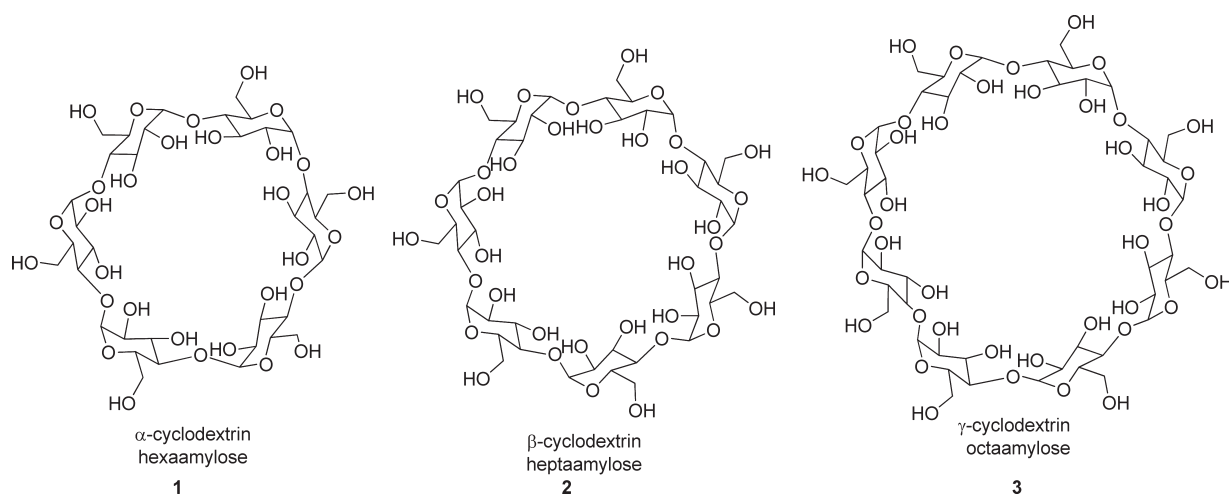


Figure 3. Structures of the commonly used α , β , and γ -cyclodextrin.

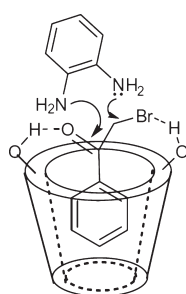
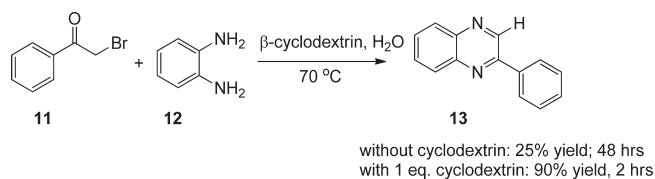


Figure 4. Proposed reaction mechanism for the synthesis of quinoxaline in the presence of β -cyclodextrin (reprinted from ref 28).

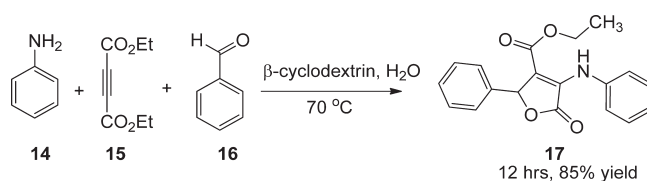


Equation 3: Synthesis of quinoxaline **13** from benzene-1,2-diamine **12** and phenacyl bromide **11**

The authors attribute this rate acceleration to the binding of phenacyl bromide in cyclodextrin, which activates it for nucleophilic attack by the diamine. A proposed mechanistic pathway is shown in Figure 4. In this model, both the bromide and carbonyl groups of compound **11** form hydrogen bonds to cyclodextrin, which make them more susceptible to nucleophilic attack by the amine moieties.

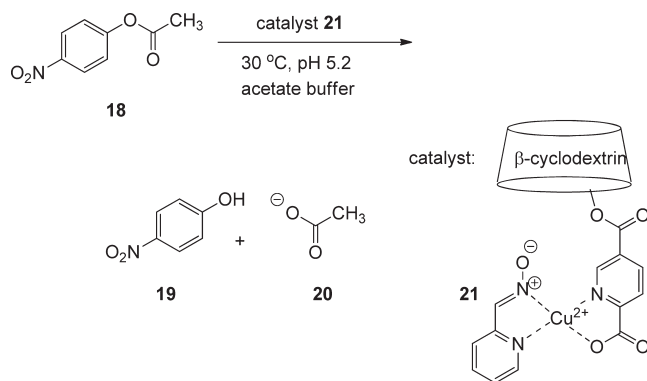
The same research group also reported that β -cyclodextrin accelerates the synthesis of furan-2(*5H*)-one **17** (eq 4),⁵⁸ which proceeds in 85% yield in the presence of 10 mol % of β -cyclodextrin. In the absence of β -cyclodextrin, no reaction occurred. In this case, cyclodextrin can be recovered and reused. In these examples, researchers used water as the reaction solvent rather than more traditional toxic organic solvents.

Covalently modified cyclodextrins have also been used as effective catalysts for a variety of reactions. For example, a copper(II)–cyclodextrin adduct (compound **21**) efficiently catalyzed the hydrolysis of *p*-nitrophenyl acetate **18** (eq 5).⁵⁹ The reaction proceeded six times faster in the presence of catalyst **21**



Equation 4: Synthesis of furanone **17** in the presence of β -cyclodextrin

compared with the reaction with a copper(II) complex that lacked cyclodextrin. Cyclodextrin played a beneficial role by binding the substrate in its hydrophobic cavity.

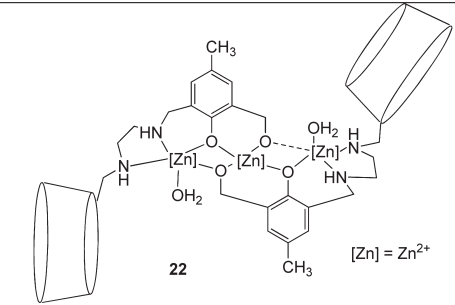
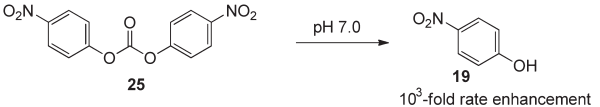
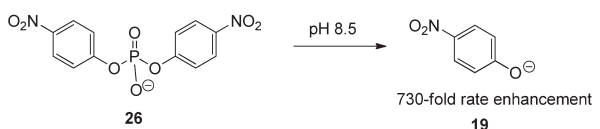
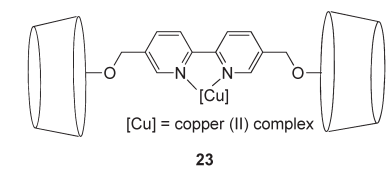
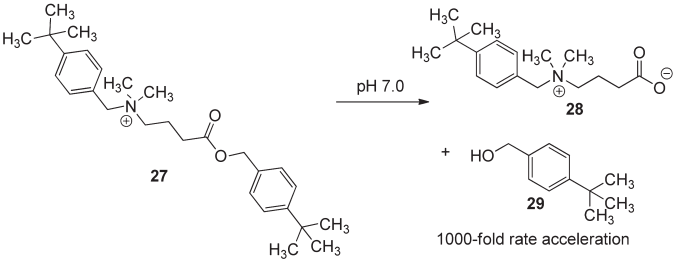
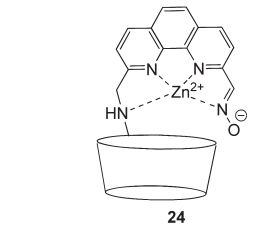
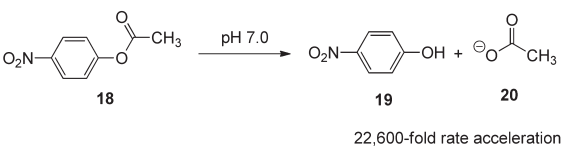


Equation 5: Hydrolysis of *p*-nitrophenyl acetate **18** in the presence of copper-cyclodextrin complex **21**

This cyclodextrin–copper catalyst was the first complex to be called an “artificial enzyme.” Such metal–cyclodextrin complexes are designed to mimic natural metalloenzymes, including esterases,⁶⁰ nucleases, and phospholipases.⁶¹ Some examples of cyclodextrin–metal complexes and the reactions they catalyze are shown in Table 1.^{62–64}

IIIc. Cyclodextrin-Based P450 Mimics. An interesting class of metal–cyclodextrin complexes are those that mimic cytochrome P450 enzymes.⁶⁵ P450 enzymes catalyze a variety of biological oxidations and are involved in ~75% of all metabolic processes.⁶⁶ Structurally, all P450 enzymes contain a heme cofactor in their active site (Figure 5), which is involved in the complex oxidation pathway.

Table 1. Organic Reactions Catalyzed by β -Cyclodextrin-Metal Complexes

macromolecular compound	Key reaction
 <p>22 [Zn] = Zn²⁺</p>	 <p>25 $\xrightarrow{\text{pH } 7.0}$ 19 10³-fold rate enhancement</p>  <p>26 $\xrightarrow{\text{pH } 8.5}$ 19 730-fold rate enhancement</p>
 <p>23 [Cu] = copper (II) complex</p>	 <p>27 $\xrightarrow{\text{pH } 7.0}$ 28 + 29 1000-fold rate acceleration</p>
 <p>24</p>	 <p>18 $\xrightarrow{\text{pH } 7.0}$ 19 + 20 22,600-fold rate acceleration</p>

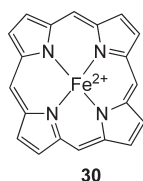


Figure 5. Structure of an unsubstituted heme cofactor 30.

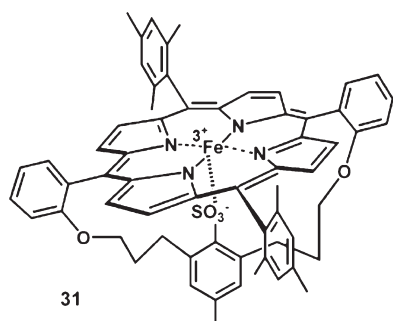
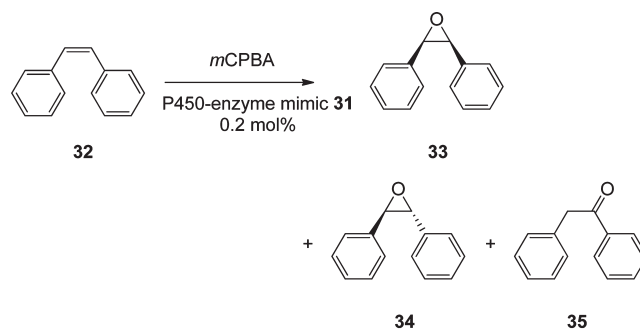


Figure 6. An iron-containing P450 enzyme mimic (reprinted from ref 69).

Most artificial P450 mimics replace the iron center with a more stable metal, such as manganese⁶⁷ or rhodium.⁶⁸ One example of

an iron-containing mimic is shown in Figure 6.⁶⁹ This compound contains a sulfonate axial ligand that mimics the cysteine axial ligand in the native enzyme.⁷⁰ The nature of the axial ligand has a dramatic effect on the reactivity of P450 mimics, likely because the axial ligand stabilizes the high oxidation states of the metal center. Compound 31 catalyzes the oxidation of *cis*-stilbene 32 with *meta*-chloroperbenzoic acid (*m*CPBA) to generate a mixture of oxidized products (compounds 33–35) (eq 6).

Equation 6: Oxidation of *cis*-stilbene 32 with iron-containing P450 mimic 31

Natural P450 enzymes exhibit remarkable regioselectivity in the oxidation of complex biological substrates. For instance, a key

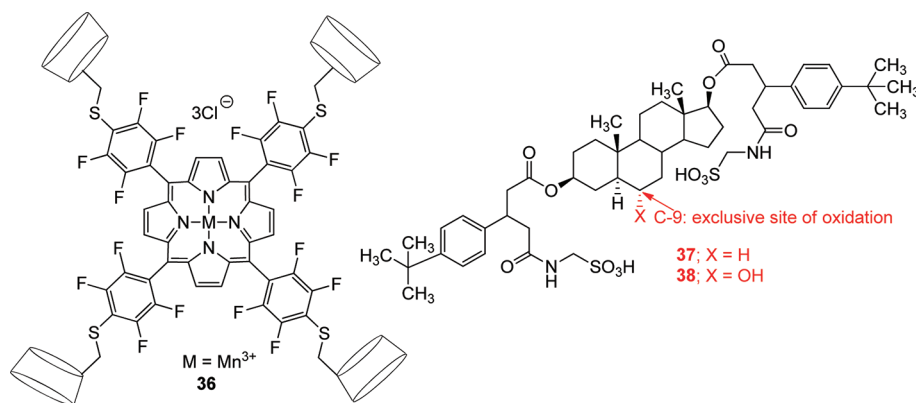


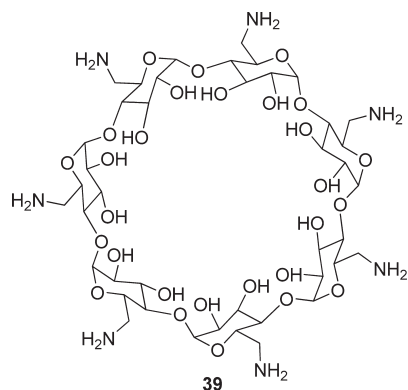
Figure 7. Cyclodextrin–porphyrin catalyst **36** and the *tert*-butyl-containing substrate **37**.

step in the biosynthesis of cholesterol⁷¹ is the selective triple oxidation of the triterpene lanosterol catalyzed by cytochrome P450. In this reaction, three saturated methyl groups are oxidized preferentially over the more reactive carbon–carbon double bonds. The ability of the enzyme to override the intrinsic reactivity of the molecule is attributed to the geometric rigidity of the enzyme–substrate complex, which dictates the regioselectivity of the oxidation.

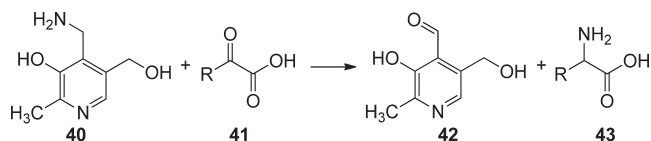
There have been numerous attempts to mimic such selectivity in synthetic systems. Breslow and co-workers synthesized a manganese–porphyrin complex, **36**, which contains four β -cyclodextrin substituents (Figure 7).⁷² The two *tert*-butyl substituents of substrate **37** bind in β -cyclodextrin with high affinity. Once the substrate binds to the porphyrin–cyclodextrin complex, hydrogen peroxide is used to selectively oxidize the C-9 position to obtain product **38**. There are several other functional groups in the molecule that are more easily oxidized, including tertiary C–H bonds and phenyl groups; however, the rigid complex positions C-9 directly above the metal center. This system also demonstrated improved catalytic efficiency compared with earlier systems, likely because of the extra stability conferred by the perfluorophenyl groups.^{73,74}

IId. Enantioselective Catalysis. There have been some attempts to achieve enantioselective catalysis using cyclodextrins; however, most of these efforts have yielded products with modest enantioselectivities.

In one example, high enantioselectivities (up to 99%) and up to 99% yield were obtained using *per*-amino- β -cyclodextrin (compound **39**) as a catalyst for the Henry reaction.⁷⁵ In this case, the chiral amino moieties are able to efficiently induce chirality in the products. To obtain optimal results, compound **39** was used in a 100% molar ratio; however, the catalyst could be recovered and reused several times with no noticeable loss of activity.



Another reaction that can be catalyzed by cyclodextrin is the transamination reaction of ketoacids to amino acids. The general transamination reaction is shown in eq 7. The pyridoxamine cofactor (compound **40**) functions as a nitrogen source in the newly formed amino acid product **43**. A detailed mechanism of the transamination reaction is discussed later in this review.



Equation 7: Transamination of a pyruvic acid **41** to an amino acid **43** with simultaneous conversion of pyridoxamine **40** to pyridoxal **42**

Breslow and co-workers found that a covalent pyridoxamine–cyclodextrin complex catalyzed the conversion of phenylpyruvic acid (compound **41**; R = benzyl) to phenylalanine (compound **43**; R = benzyl) with an enantiomeric ratio of 5:1 L:D.⁷⁶ Later modifications increased the ratio up to 6.8:1.⁷⁷ Other research groups reported extremely high enantiomeric excesses (ee's) using pyridoxamine–cyclodextrin conjugates;⁷⁸ however, their experimental results could not be duplicated.⁷⁹

III. CUCURBITURILS

IIIa. Introduction. Cucurbiturils (CBs) are another class of macrocycles that can bind a variety of small-molecule guests.⁴⁴ These macrocycles are composed of glycoluril repeat units connected via methylene bridges. CBs are named by the number of monomers they contain, i.e. CB[6] refers to a CB with six glycoluril units.

CB[6] (compound **46**) was first synthesized by condensing formaldehyde **45** with glycoluril **44** in concentrated sulfuric acid in 1905 (eq 8), although the product structure was not elucidated until 1981.⁸⁰ Milder synthetic methods (9 M sulfuric acid at 75 °C) led to the formation of a mixture of CB isomers: CB[6] (60% yield), CB[5] (compound **47**, 10% yield), CB[7] (compound **48**, 20% yield), and other higher homologues (10% combined yield).^{81,82} The X-ray crystal structures of CB[5]–CB[8] are shown in Figure 8.

The interior cavities of CB macrocycles possess a number of features that enable them to complex small-molecule guests efficiently. CB macrocycles bind small-molecule hydrophobic guests in their hydrophobic interior cavities.⁸³ In addition, the

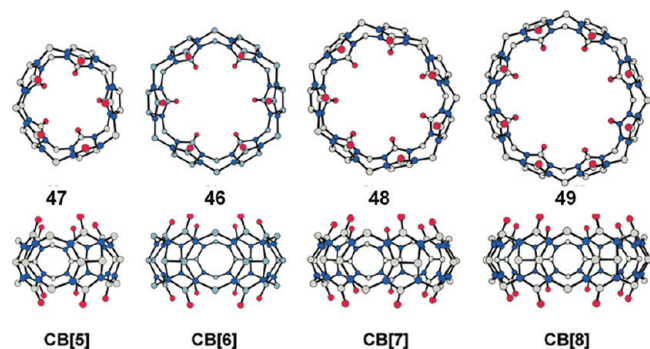
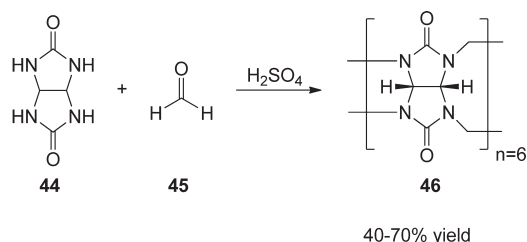


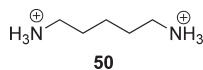
Figure 8. X-ray crystal structures of CB[n] ($n = 5-8$) (Reprinted from ref 81).



Equation 8: First reported synthesis of CB[6]

CB rims are lined with carbonyl groups, which can stabilize cationic moieties, such as transition metal cations⁸⁴ and quaternary ammonium salts.⁸⁵

Molecules that are both hydrophobic and cationic bind in CB with very high affinities. For example, the alkylated ammonium dication cadaverine (compound **50**) binds in CB[6]⁸⁶ and CB[7]⁸⁷ with very high affinities. The alkyl chain of cadaverine spans the interior hydrophobic cavity, and both ammonium groups bind to a carbonyl-lined rim.



IIIb. Catalysis. CB macrocycles can accelerate the reactions of small-molecule guests that bind in the interior. For example, CB[6] and CB[7] accelerate the hydrolysis of compounds **51**, **53**, and **55** (Table 2).⁸⁸ These compounds contain cadaverine, phenyl moieties, or both, which bind in CB cavities. Only modest rate accelerations were obtained in reactions 1 and 2, which may be due to the acidic reaction conditions that destroy the integrity of the CB cavity. The hydrolysis of oxime **55**, by contrast, proceeded with a 285-fold rate acceleration in the presence of CB[7].

Unfortunately, product inhibition was observed in these reactions because the products have a higher binding affinity for CB than the reactants.

¹H NMR Analysis: Binding of small molecules in CB (and in many other macrocycles) leads to substantial changes in the ¹H NMR spectrum due to changes in the local environment. For example, the cadaverine moiety of compound **51** binds in CB[6], which causes a substantial upfield shift (−0.45 ppm) of those proton signals (Figure 9). The aromatic protons, which do not bind in the macrocycle, have a much smaller proton shift (−0.05 ppm).

The NMR spectrum can thus be used to determine which part of the molecule is encapsulated by the macrocycle. Similar proton

shifts have been observed in all cases in which CB binds small-molecule guests.⁸⁹ Reaction rates can also be determined by monitoring the disappearance of the encapsulated starting material by ¹H NMR.⁹⁰

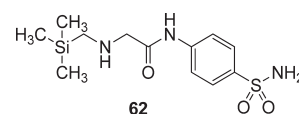
CB[8] has a large internal cavity (479 Å³) that enables it to bind two small-molecule guests simultaneously.⁹¹ For example, a variety of *trans*-cinnamic acids (compounds **57**) form 2:1 complexes with CB[8] (Chart 1).⁹² After binding, the compounds undergo a photodimerization reaction in the CB cavity that forms the head–head *syn* dimer **58**. (Scheme 1, reaction 1). In contrast, irradiating *trans*-cinnamic acid in an aqueous solution caused complete isomerization of the olefin (reaction 2), and performing the same reaction in the solid state led to formation of the anti dimer (reaction 3).

In this case, CB[8] acts as a microreactor that binds the compounds in a *syn* geometry. Calculations indicate that this geometry fits well in the CB[8] cavity. An anti arrangement of the molecules, by contrast, requires a significant fraction of the small molecule to protrude from the cavity (Figure 10).

Researchers exploited the high affinities of CB for small-molecule guests⁹³ to design a thermodynamically driven molecular shuttle.⁹⁴ A schematic illustration of this system is shown in Figure 11. The bifunctional molecule **61** contains both a CB[7] binding epitope (adamantane) and a carbonic anhydrase binding epitope (sulfonamide). In the absence of CB[7], compound **61** will bind to the active site of carbonic anhydrase and inhibit its activity. When CB[7] is added to the solution, it should bind to adamantane and remove compound **61** from the enzyme, thus restoring enzymatic activity.

In practice, when CB[7] was added to the complex of carbonic anhydrase and compound **61**, only 45% of the enzymatic activity was restored. This result was unexpected, because the binding affinity of CB[7] for adamantane is substantially higher than the binding affinity of carbonic anhydrase for sulfonamides ($4.1 \times 10^{12} \text{ M}^{-1}$ vs $1.08 \times 10^8 \text{ M}^{-1}$, respectively). Despite the high binding affinity of CB[7] for adamantane, the slow kinetics of complex formation prevented the complete restoration of enzymatic activity.

When adamantane was replaced with a trimethylsilyl group (compound **62**) and a similar experiment was performed, 87% of enzymatic activity was restored. Even though CB[7] has a lower binding affinity for the trimethylsilyl epitope, the faster binding kinetics led to this successful result.



IV. METAL-DIRECTED MACROCYCLES

IVa. Introduction. Molecular self-assembly occurs frequently in biological systems.^{95,96} For example, a mammalian cell can be viewed as a noncovalent self-assembly of complex biological molecules.⁹⁷ Nature uses a variety of weak forces⁹⁸ to guide such self-assembly, including van der Waals attractions and hydrophobic binding.

In addition to these weak attractive forces, synthetic self-assembled compounds can utilize metal–ligand complexation as an additional binding force. Because metal–ligand bond formation is reversible, such bonds can repeatedly break and re-form until the most stable structure is reached. Self-assembled

Table 2. Reactions catalyzed by CB[6] and/or CB[7]

Reaction:	Rate acceleration:
Reaction 1 	4-fold acceleration
Reaction 2 	29-fold acceleration
Reaction 3 	285-fold acceleration

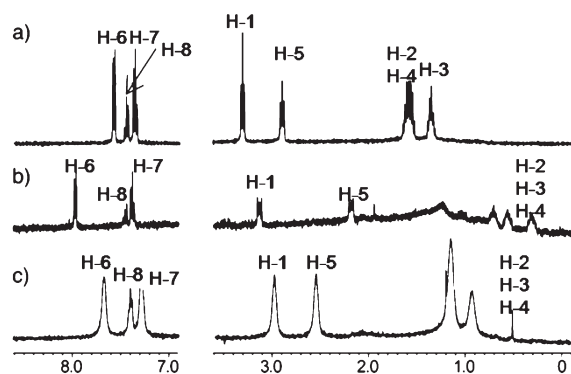


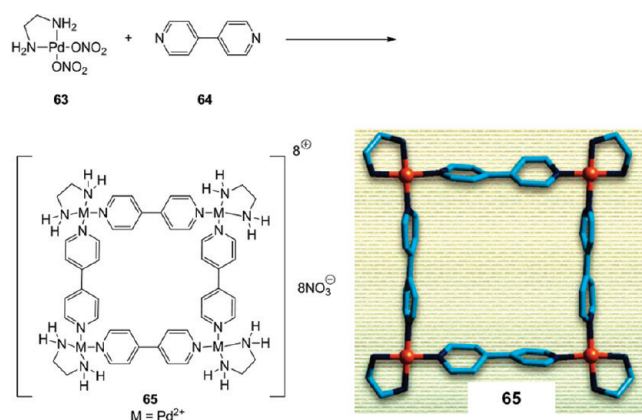
Figure 9. ^1H NMR of compound 51 (a) in D_2O ; (b) with 1.5 equiv of CB[6]; and (c) with 2 eq of CB[7] (reprinted from ref 88).

organometallic complexes have been extensively studied by the research groups of Makoto Fujita,⁹⁹ Peter Stang,¹⁰⁰ and Kenneth Raymond,¹⁰¹ and the biomimetic catalytic properties of these complexes have been investigated.

IVb. Catalysis. Fujita and co-workers¹⁰² reported the first synthesis of a self-assembled molecular square (compound 65) via palladium-directed self-assembly (eq 9).¹⁰³ The compound was formed in quantitative yield by mixing the palladium complex 63 with bipyridine (compound 64). Many ligands, transition metals, and aromatic compounds were investigated; however, all other combinations yielded polymers or intractable mixtures. The successful synthesis of compound 65 is due to the kinetic lability of bipyridine that facilitated rapid and reversible bond formation. The kinetically inert ethylenediamine ligands, in the interim, were unaffected.

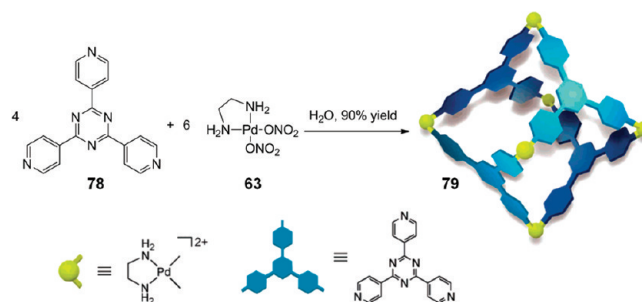
Analogous macrocycle 66, with perfluorophenyl moieties, binds electron-rich aromatic compounds with high affinities (Figure 12, Chart 2).¹⁰⁴ The electron-rich guests form a “ π -stack” sandwich with the two perfluorophenyl moieties, which stabilizes the complex.

Similarly, Stang and co-workers¹⁰⁵ reported the use of platinum and palladium molecular “clips” to direct the self-assembly of molecular squares (Figure 13).¹⁰⁶ Stang has since synthesized a wide variety of metal-coordinated self-assembled supramolecular structures, including three-dimensional nanocage architectures.^{107–109}



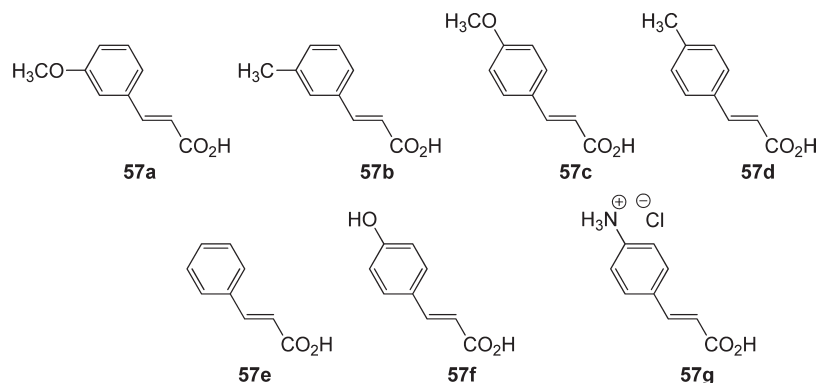
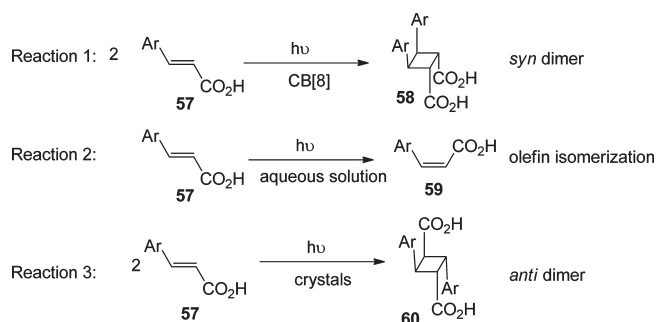
Equation 9: First synthesis of an organometallic molecular square

Metal–ligand binding can also be used to form three-dimensional nanocages. For example, Fujita and co-workers synthesized nanocage 79 by mixing a tridentate organic ligand (compound 78) with palladium complex 63 (eq 10).^{110–112} The resulting complex was isolated in 90% yield and was cocrystallized with four adamantane molecules bound in its hydrophobic interior. Larger cavities with the same geometry were synthesized by increasing the size of the tridentate organic spacer.



Equation 10: Synthesis of nanocage 79 via metal-directed self-assembly

These nanocages have a number of features that make them attractive biomimetic catalysts, including (1) ease of synthesis due to spontaneous self-assembly; (2) a large hydrophobic

Chart 1. *Trans*-Cinnamic Acids **57** Studied in the Photodimerization ReactionScheme 1. Reaction of *trans*-Cinnamic Acids **57** under a Variety of Conditions

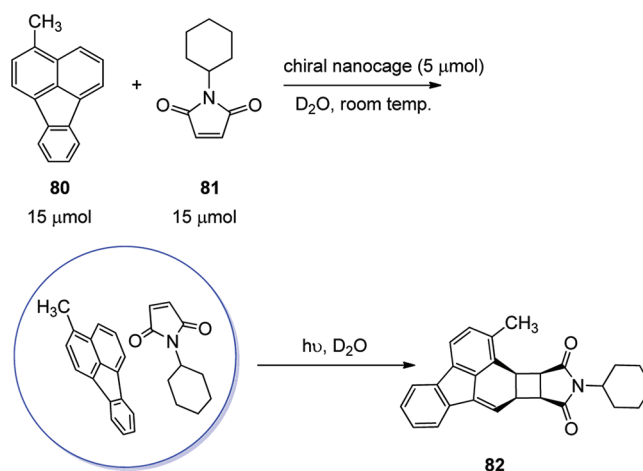
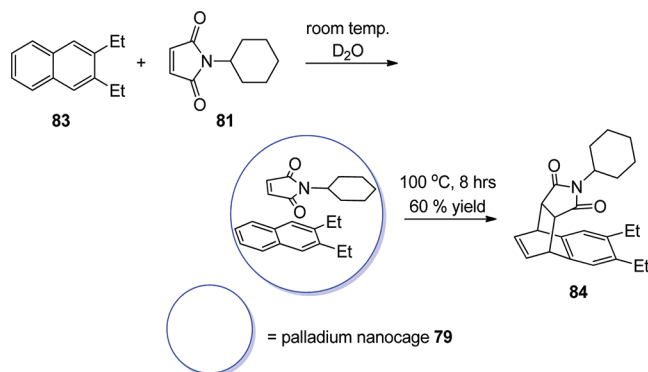
cavity, determined by the hydrophobic aromatic walls; and (3) high water solubility due to the overall positive charge.

One example of a reaction that occurred in an analogous palladium nanocage is the [2 + 2] cycloaddition of methyl-fluoranthene **80** and *N*-cyclohexyl-maleimide **81**. In this case, the palladium was substituted with external chiral ligands. Even though these ligands are the only source of chirality in the complex, the resulting product **82** was formed in 55% yield and a remarkable 50% ee (eq 11).¹¹³ Other notable features of this reaction include complete regioselectivity, despite the multitude of potential products, as well as the facile reaction of the typically unreactive fluoranthene moieties.

Palladium nanocages can also act as microreactors to direct the regioselectivity of reactions. For example, the Diels–Alder reaction of naphthalene **83** and maleimide **81** proceeded exclusively at the unsubstituted, less electron-rich aromatic ring (eq 12).¹¹⁴ In contrast, normal Diels–Alder reactions preferentially occur on the more electron-rich ring. This unusual regioselectivity is due to the geometry of the encapsulated substrates, which positions the maleimide dienophile above the unsubstituted ring (Figure 14).

Similarly, compound **85** underwent a Diels–Alder reaction at one of its terminal rings rather than at the more reactive central ring (eq 13).¹¹² Other examples of unusual regioselectivities caused by tight binding in Fujita's nanocage have also been reported.^{115–117}

Similarly, Raymond and Bergman reported the synthesis of organometallic tetrahedral nanocages with the general formula

Equation 11: Cycloaddition of methyl-fluoranthene and *N*-cyclohexyl-maleimide catalyzed by a palladium nanocageEquation 12: Diels–Alder reaction of diethylnaphthalene **83** and *N*-cyclohexyl-maleimide **81** in palladium nanocage **79**

M_4L_6 ($\text{M} = \text{Ga}^{3+}, \text{Al}^{3+}, \text{In}^{3+}, \text{Fe}^{3+}$; $\text{L} = \text{bis-catechol naphthalene}$) (Figure 15),¹¹⁸ which assembled spontaneously by mixing the metal and the ligand in the appropriate stoichiometric ratios. These complexes are also inherently chiral as a result of the ligand

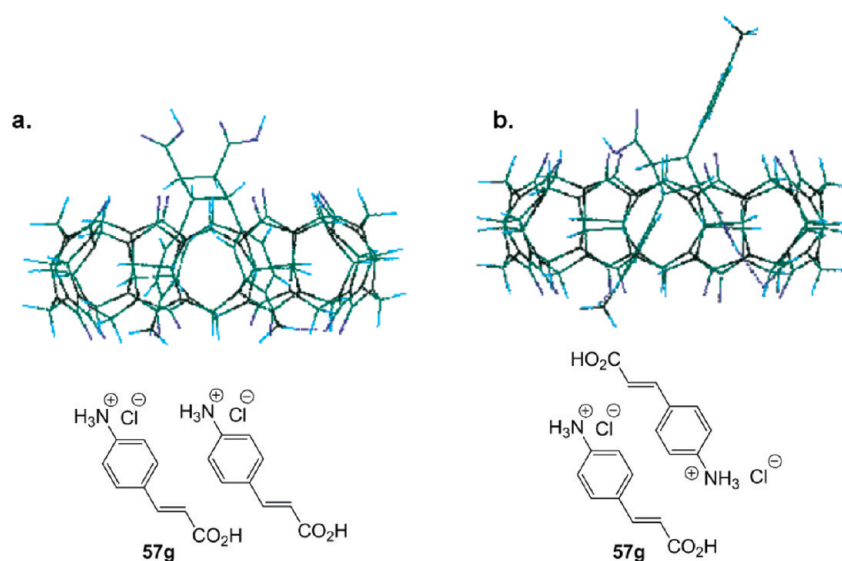


Figure 10. Energy-minimized structure of the (a) syn head–head dimer of *trans*-4-aminobenzoic acid (compound **57g**); and (b) anti head–tail dimer of *trans*-cinnamic acid in CB[8] (reprinted from ref 92).

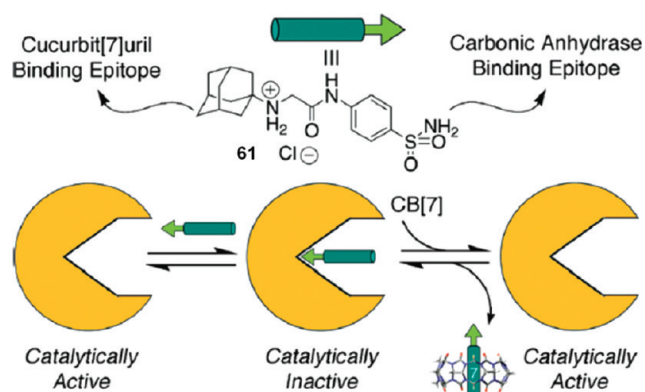


Figure 11. Schematic illustration of how bifunctional epitope **61** controls the activity of carbonic anhydrase (reprinted from ref 94).

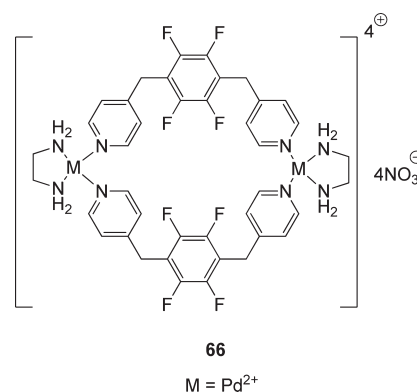
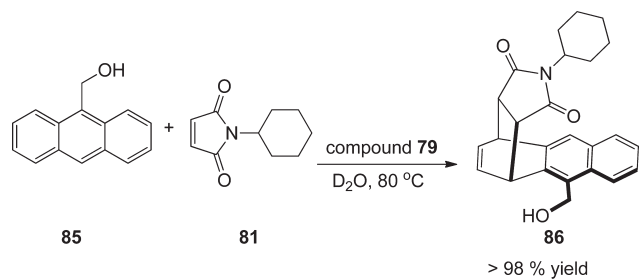


Figure 12. Perfluorophenyl analogue **66**.



Equation 13: Diels-Alder reaction of 9-anthracenemethanol and *N*-cyclohexyl-maleimide in a palladium nanocage

arrangement around the metal center, and the two enantiomers can be separated by crystallization.^{119,120}

The Ga₄L₆ tetrahedron has been used as a “nanoreactor” to catalyze a variety of organic transformations. This nanocage catalyzes reactions by stabilizing cationic intermediates such as iminium cations, transition metal cations,¹²¹ diazonium cations, and tropylium cations,¹²² which lowers the activation energy of the overall reaction. Moreover, product inhibition can generally

be avoided in these cases by choosing reactions in which the product binding affinity is lower than the reactant binding affinity.

For example, Raymond and Bergman reported that the Nazarov cyclization of pentadienol **88** could be catalyzed by 7 mol % of the tetrahedral Ga₄L₆ host **87** (Scheme 2).¹²³ This reaction proceeded 6 orders of magnitude faster in the presence of the catalyst, which is due to the ability of the nanocage to stabilize cationic intermediate **93** (Scheme 3). Moreover, binding inside the nanocage restricts the free rotation of reactant **88**, which lowers the enthalpic activation barrier. To avoid potential product inhibition, the initial product **89** was immediately reacted with maleimide to yield Diels–Alder adduct **91**, which does not bind appreciably in the macrocycle.

Other examples of reactions catalyzed by nanocage **87** are shown in Table 3,^{124–126} and the proposed catalytic cycle for reaction 3 is shown in Figure 16. In this reaction, the aza-Cope rearrangement (which is the rate-determining step) occurs inside the nanocage. The resulting iminium then undergoes hydrolysis in aqueous solvent to yield the final aldehyde product.

Enantioselective catalysis is also possible using single enantiomers of the Ga₄L₆ nanocage that have been separated by crystallization.

Chart 2. Association Constants for Small-Molecule Guests Bound in Self-Assembled Macrocycle 66

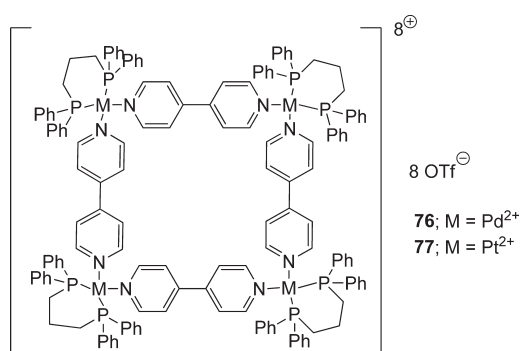
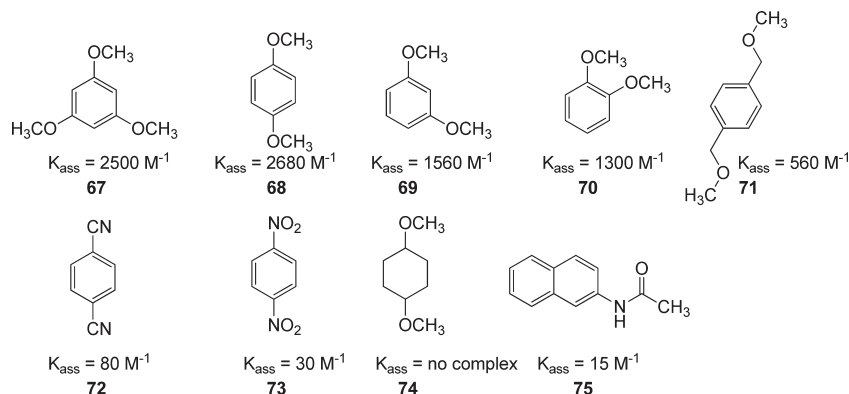


Figure 13. Self-assembled macrocycles 76 and 77 synthesized by Stang and co-workers.

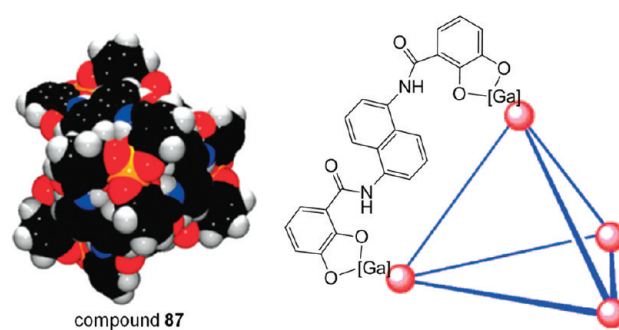
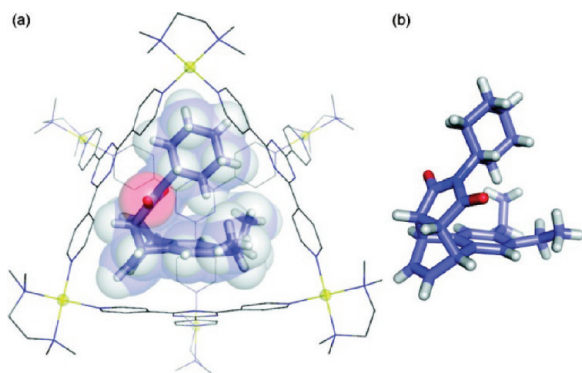
Figure 15. Space-filling model of a Ga_4L_6 tetrahedron (compound 87) (left) and a schematic depiction of the structure (right) (reprinted from ref 118).

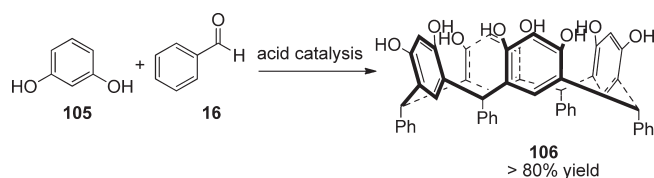
Figure 14. Crystal structure of the palladium nanocage complexed with product 84 (reprinted from ref 114).

For example, the enantioselective aza-Cope rearrangement of compound 103 proceeded in the presence of the homochiral nanocage to generate products 104 with up to 78% ee (Scheme 4).¹¹⁹ Less sterically bulky substrates led to lower ee's because they formed looser complexes with the chiral nanocage.

V. SYNTHETIC CAVITANDS

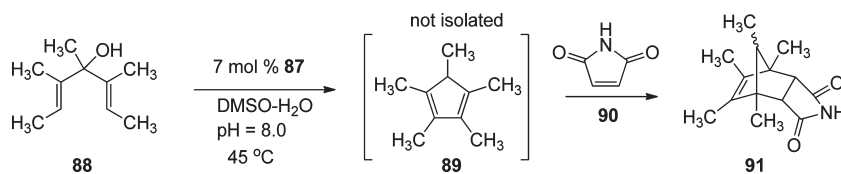
Va. Introduction. The use of synthetic cavitands for biomimetic catalysis has been extensively investigated, most notably by

Julius Rebek and co-workers.¹²⁷ The cavitands studied by Rebek are synthesized from resorcinarene (compound 106), which is itself formed from the condensation of benzaldehyde and resorcinol 105 (eq 14).^{128,129} Although numerous products are theoretically possible, the desired tetramer was formed in more than 80% yield.

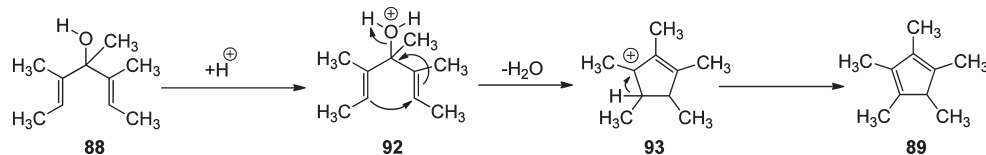


Equation 14: Synthesis of resorcinarene from resorcinol and benzaldehyde

Resorcinarene adopts a shallow vase-like conformation, with the phenyl rings oriented down and the hydroxyl groups lining the upper cavity rim. Although the unfunctionalized cavity is too shallow to encapsulate small-molecule guests, the hydroxyl groups can be functionalized to deepen the cavity. For example, condensation of resorcinarene 106 with 1,2-difluoro-4,5-dinitrobenzene 107 yields the tetraphenyl-functionalized cavitand 109 and triphenyl-substituted compound 108 (eq 15). Like resorcinarene, these extended cavitands contain a hydrophobic bottom portion (from the phenyl groups) and a highly polar functionalized rim (with nitro and hydroxyl substituents).

Scheme 2. Nazarov Cyclization Catalyzed by Ga₄L₆ Nanoreactor 87

Scheme 3. Mechanism of the Nazarov Cyclization Reaction

Table 3. Examples of Reactions Catalyzed by the Nanocage Ga₄L₆

Reaction 1	orthoformate hydrolysis	$\text{RO-CH(OR)-OR} + \text{H}_2\text{O} \xrightarrow[\text{pH 11}]{1 \text{ mol \% } 87} \text{H-C(=O)-OR} + 2 \text{ROH}$ $\text{H-C(=O)-OR} + \text{OH}^- \rightarrow \text{H-C(O}^-\text{)-OR} + \text{H}_2\text{O}$ $\text{H-C(O}^-\text{)-OR} + 2 \text{ROH} \rightarrow \text{H-C(O}^-\text{)-OR} + 3 \text{ROH}$	R = Me, Et, <i>i</i> Pr, <i>n</i> -Bu, <i>i</i> -Bu quantitative yield
Reaction 2	acetal hydrolysis	$\text{H}_3\text{CO-C(OCH}_3\text{)}_2\text{-R}_2 \xrightarrow[\text{pH 10, H}_2\text{O}]{5 \text{ mol \% } 87} \text{H}_3\text{CO-C(=O)-R}_2 + 2 \text{CH}_3\text{OH}$	yield > 95% for R groups that bind in the nanocage
Reaction 3	Aza Cope rearrangement	$\text{H}_3\text{C-N}^+\text{=C(CH}_3\text{)-C}\equiv\text{C-R} \xrightarrow[\text{H}_2\text{O}]{60 \text{ }^\circ\text{C}} \text{H}_3\text{C-N}^+\text{=C(CH}_3\text{)-C=C-R} \xrightarrow{\text{H}_2\text{O}} \text{H}_2\text{C=C(CH}_3\text{)-R} + \text{H}_3\text{C-NH}_2$	

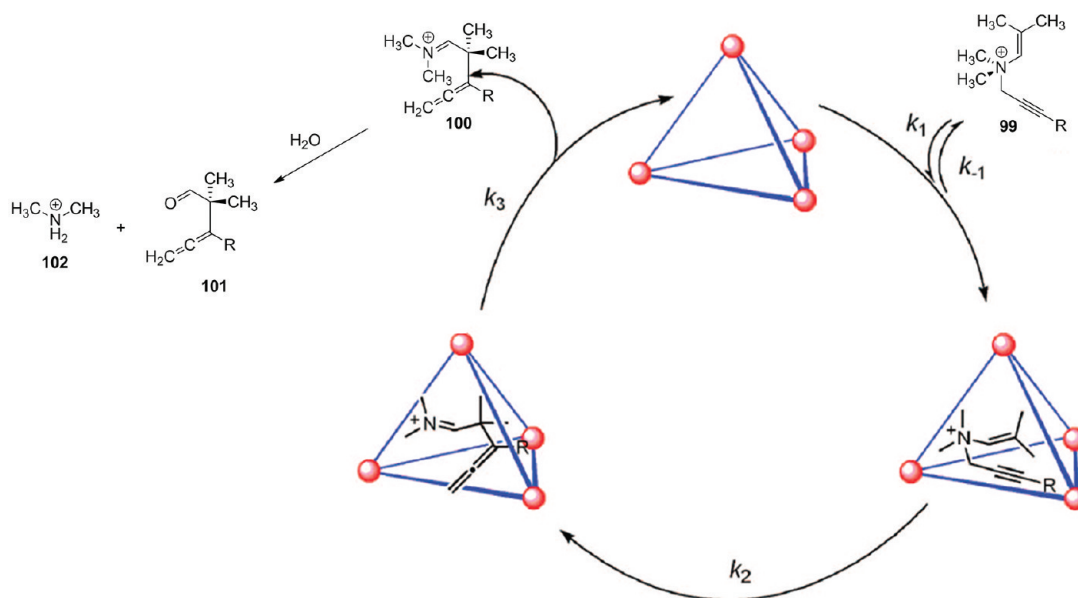
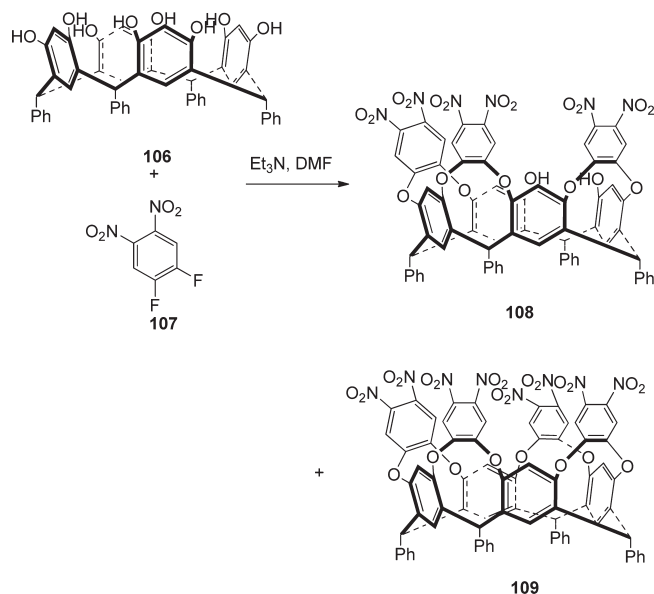


Figure 16. Mechanism of an aza-Cope rearrangement that occurs in tetrahedral nanocage 87 (reprinted from ref 126).

The nitro groups of compound **109** can be further functionalized in a number of ways, for example, by reducing them to amino groups.^{130–132} Moreover, triphenyl compound **108** was reacted further at the unsubstituted hydroxyl groups to yield monofunctionalized synthetic cavitands **110**, **111**, and **112**.^{133–135} (Chart 3).

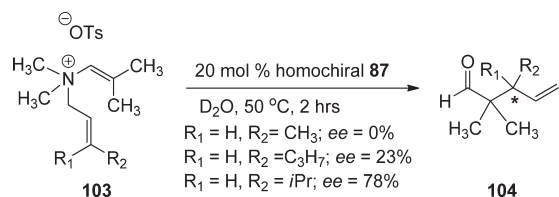
Vb. Catalysis. Resorcinarene-derived cavitands have been used as supramolecular catalysts for a variety of reactions. For example, the Diels–Alder reaction of *N*-cyclooctyl-maleimide **115** and 9-anthracenemethanol **85** proceeded 57 times faster in the presence of cavitant **119** than the uncatalyzed reaction (Scheme 5).¹³⁶ Other substituted maleimides also demonstrated significant rate enhancements that correlated with the binding affinity of the cycloalkane substituent in the cavitant.

The synthetic cavitant accelerates this Diels–Alder reaction via dual activation of the dienophile: the bulky substituents bind in the cavitant core, and the cavitant amides form hydrogen



Equation 15: Synthesis of cavity-extended resorcinarenes **108** and **109** by nucleophilic aromatic substitution

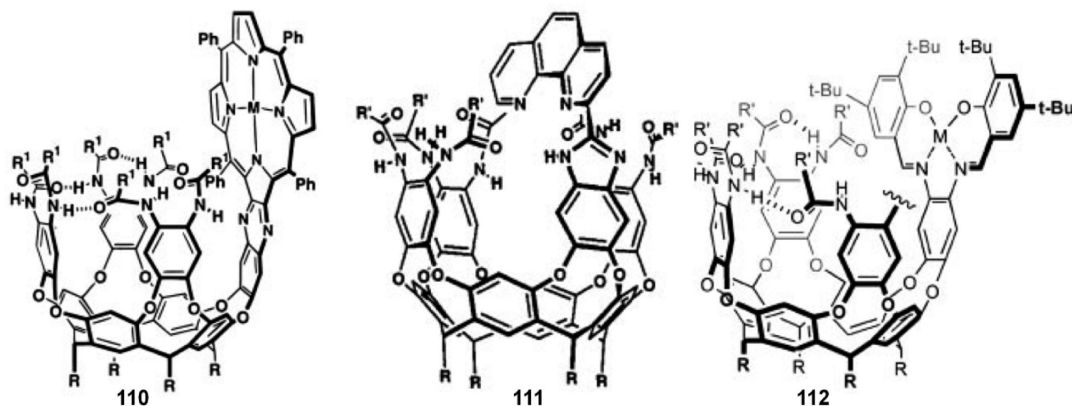
Scheme 4. Enantioselective Synthesis of Aldehydes **104** via an aza-Cope Rearrangement



bonds with the maleimide carbonyls. Other examples of reactions catalyzed by synthetic cavitands are shown in Table 4.^{135,137,138}

Figure 17 shows the energy-minimized geometry of compound **113** in cavitant **119**. Because the Diels–Alder product is

Chart 3. Mono-Functionalized Synthetic Cavitands



Scheme 5. Diels–Alder Reactions of Alkyl-Substituted Maleimides and 9-Anthracenemethanol in Cavitant **119**

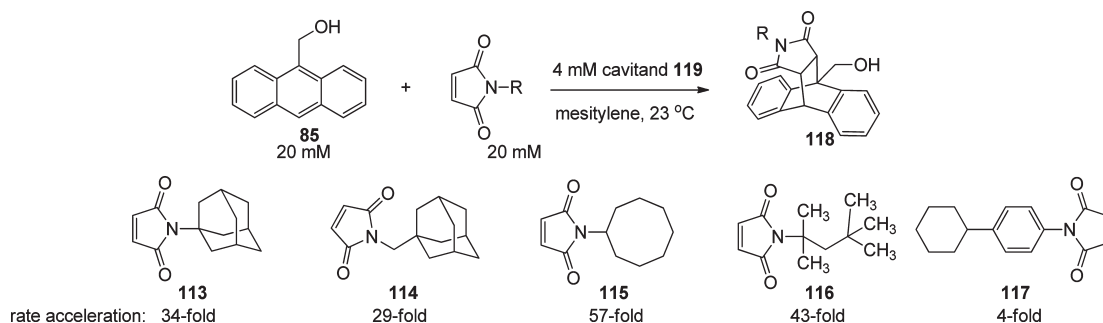


Table 4. Examples of Organic Reactions Catalyzed by Synthetic Cavittands

Reaction 1	1,3-dipolar cycloaddition			240-fold acceleration at 298 K
Reaction 2	carbonate hydrolysis			
Reaction 3	Nucleophilic aromatic substitution			400-fold rate acceleration at 300 K

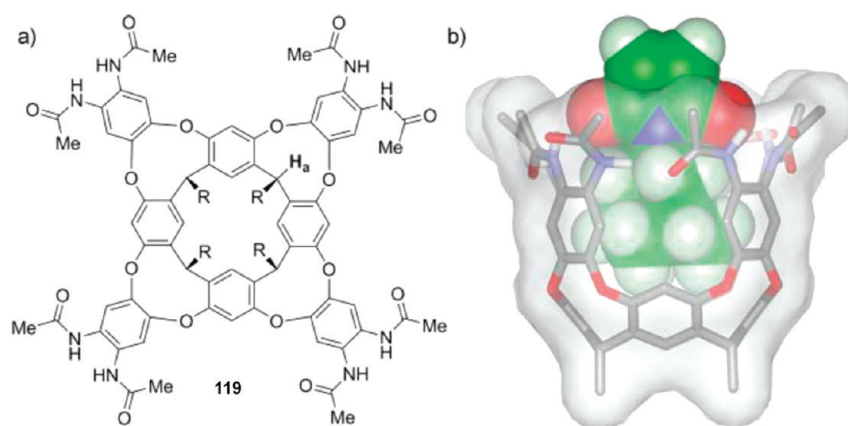
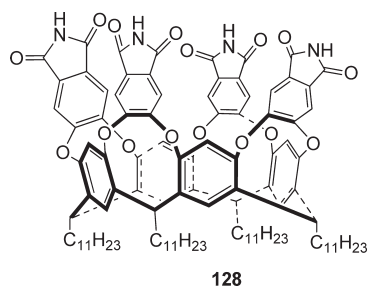


Figure 17. (a) Structure of the synthetic cavittand used in the Diels–Alder reaction and (b) crystal structure of compound **113** in cavittand **119** (reprinted from ref 136).

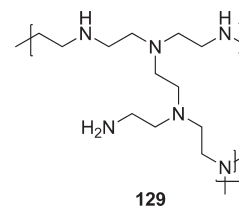
highly sterically hindered, it does not bind in the cavittand, and no product inhibition is observed.



VI. POLYETHYLENIMINE-BASED CATALYSIS

Vla. Introduction. Polyethyleneimine (PEI) is a commercially available polymer, with molecular weights between 1300 and 750 000 g/mol. The general structure of PEI is shown below (compound **129**). It has a highly branched structure: 25% of the nitrogens are primary, 25% are tertiary, and 50% are secondary. The nitrogens of PEI titrate over a broad pH range (3–13), which means that at any intermediate pH, the polymer has both protonated and unprotonated amines.¹³⁹ This feature

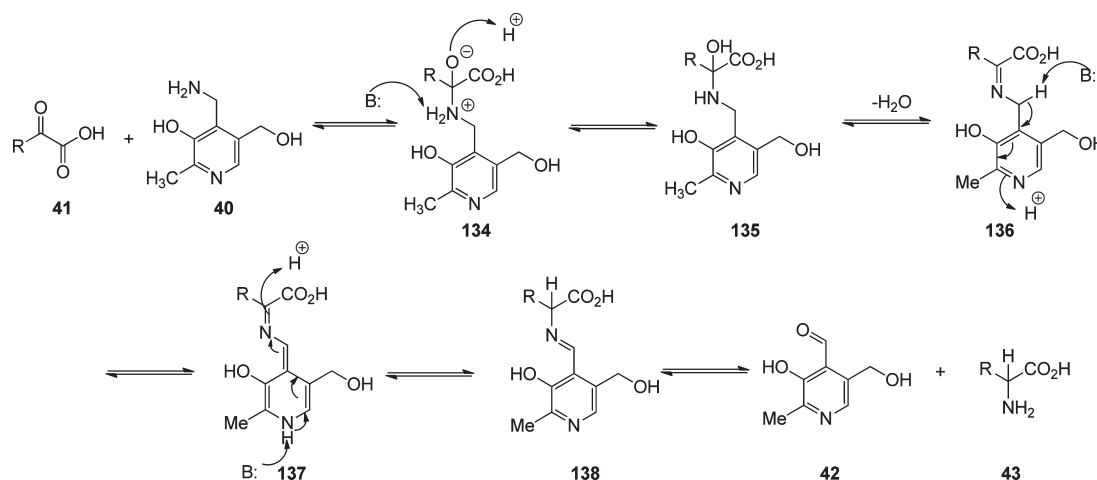
allows PEI to be used as a general acid–general base catalyst for a variety of reactions.^{140,141}



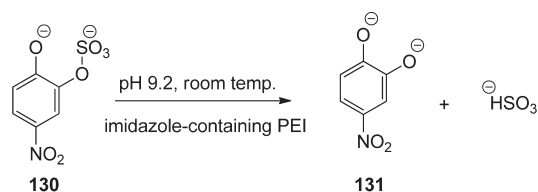
Commercially available PEI can be covalently modified to increase its hydrophobicity. For example, PEI was alkylated with dodecyl iodide to yield a partially laurylated hydrophobic polymer.^{142,143} The amino groups were also reductively methylated¹⁴⁴ and acylated.^{145,146}

Vlb. Catalysis. One of the first examples using PEI as a supramolecular catalyst was reported by Irving Klotz in 1971.¹⁴⁷ Klotz attached long dodecyl chains to increase PEI's hydrophobicity, as well as basic imidazole side chains. The polymer accelerated the hydrolysis of 2-hydroxy-5-nitrophenyl-sulfate (compound **130**) to 4-nitrocatechol (compound **131**), which proceeded 10^{12} times faster in the presence of the polymer compared with the reaction catalyzed by free imidazole

Scheme 6. Mechanism of the transamination reaction between pyridoxamine 40 and a ketoacid substrate 41 (acid- and base-catalyzed steps are denoted with H^+ and B:, respectively)

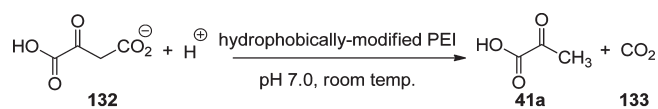


(eq 16).¹⁴⁸ This complex was called a “synzyme”, meaning a synthetic enzyme.



Equation 16: Hydrolysis of 2-hydroxy-5-nitrophenylsulfate to 4-nitrocatechol catalyzed by a modified PEI catalyst

Following this initial report, many other examples have been reported in which PEI accelerates the rate of organic reactions. One example is the decarboxylation of oxalacetic acid **132**, which proceeded $\sim 10^5$ times faster in the presence of the catalyst compared with the polymer-free reaction (eq 17).⁹

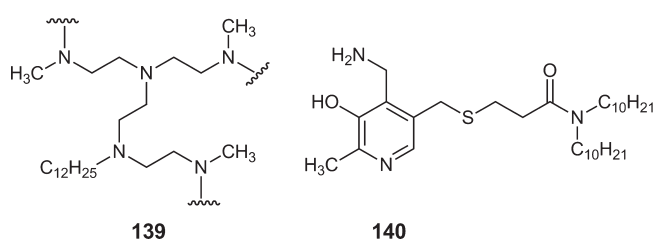


Equation 17: Decarboxylation of oxalacetic acid catalyzed by PEI

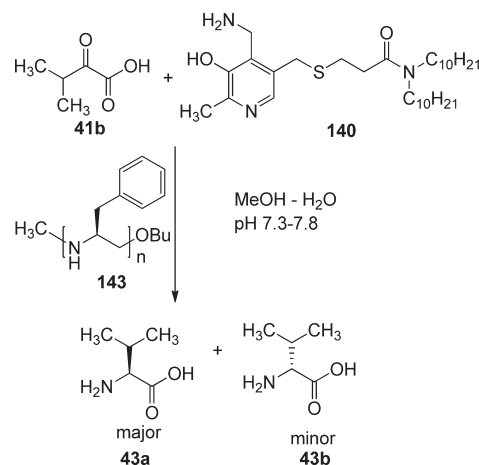
Similarly, the transamination of ketoacids **41** to amino acids **43**, which involves a series of acid- and base-catalyzed steps, can be catalyzed by PEI. The mechanism is shown in Scheme 6. The ketoacid substrate forms an initial Schiff base with pyridoxamine cofactor **40**. This ketimine Schiff base **136** is deprotonated at one carbon and reprotonated at the α -carbon to yield a new aldimine Schiff base **138**. This imine is then hydrolyzed to yield the target amino acid product **43** and pyridoxal phosphate **42**. These steps are all catalyzed in vivo by the enzyme transaminase.

Breslow and co-workers have reported the synthesis of PEI derivatives that successfully mimic the enzyme transaminase.^{149,150} In particular, hydrophobically modified PEI **139** was mixed with hydrophobically modified pyridoxamine cofactor **140** (Chart 4). This system accelerated the transamination of ketoacids to amino acids, with higher rate accelerations observed for hydrophobically

Chart 4. Hydrophobically-Modified PEI 139 and Hydrophobically Modified Pyridoxamine 140



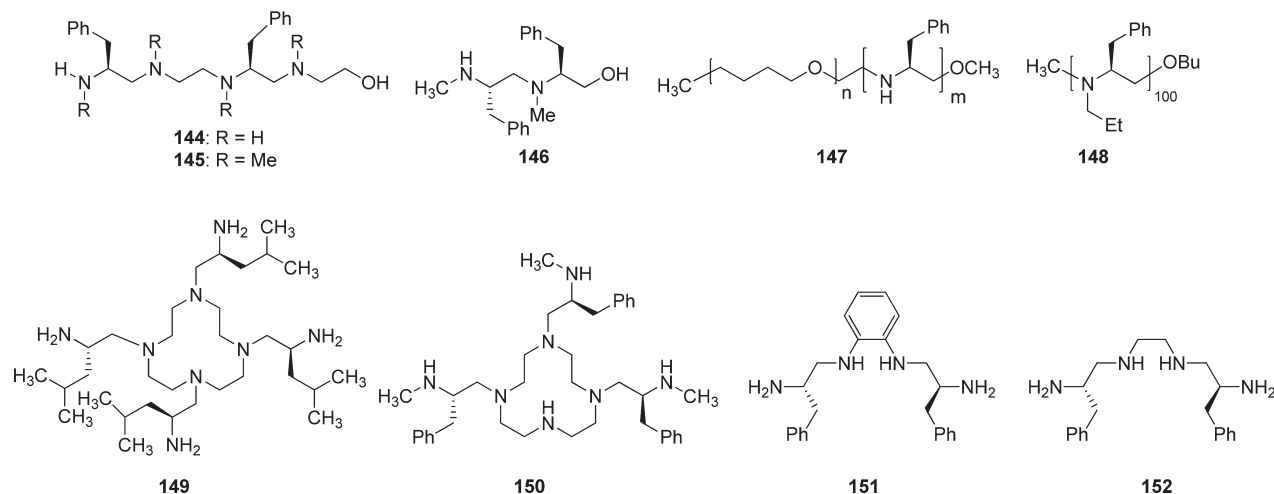
Scheme 7. Synthesis of Chiral Amino Acids Using Homo-chiral PEI



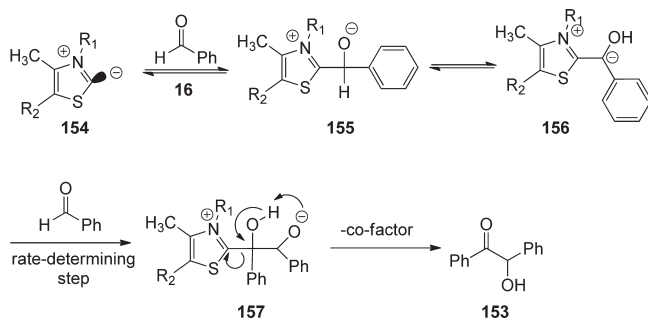
substituted ketoacids. The best rate enhancement, 725 000-fold, was observed for the transamination of indole pyruvic acid to tryptophan.⁸

These rate enhancements were substantially higher than those observed for a covalent polymer–pyridoxamine hybrid (6700-fold)¹⁵¹ because the noncovalent system is able to find the

Chart 5. Other chiral amine catalysts

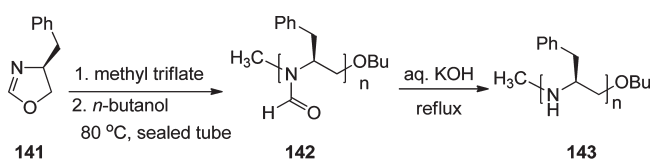


Scheme 8. Mechanism of the Thiazolium-Catalyzed Benzoin Condensation



optimal polymer–cofactor–substrate geometry. Moreover, the pyridoxamine cofactor was regenerated by using a sacrificial amino acid, phenylmethylglycine that formed acetophenone, CO₂, and the desired pyridoxamine.

Attempts to develop a polymeric system that transaminates ketoacids enantioselectively have met with only limited success. In one attempt, homochiral PEI **143** was synthesized from the cationic polymerization of 4-*S*-benzyl-oxazoline (compound **141**),^{152–154} followed by subsequent deformylation (eq 18).¹⁵⁵ This hydrophobic chiral polymer was used with hydrophobically modified pyridoxamine **140** to catalyze the transamination of 3-methyl-2-oxobutanoic acid (**41b**) to valine in up to 66% L ee (Scheme 7).

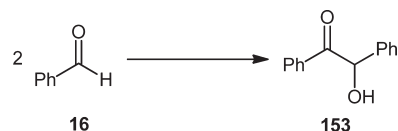


Equation 18: Synthesis of homochiral polyethyleimine

Chiral polymers that were covalently linked to pyridoxamine induced only moderate ee's in the transamination reaction, and other chiral amines performed similarly.^{156,157} Some of these

chiral amines (Chart 5) have been studied for other applications, including catalyzing a Michael reaction, solubilizing carbon nanotubes,¹⁵⁸ and complexing and delivering siRNA to cells.^{159–161}

PEI has been used to accelerate the benzoin condensation (eq 19).¹⁶² The reaction proceeded 3 orders of magnitude faster in the presence of PEI compared with the polymer-free reaction. This reaction utilizes a thiazolium-derived cofactor (compound **154**), which activates benzaldehyde via formation of a nucleophilic, carbene-like “Breslow intermediate” (compound **156**) (Scheme 8).¹⁶³ Other PEI-catalyzed reactions are summarized in Table 5.



Equation 19: The benzoin condensation

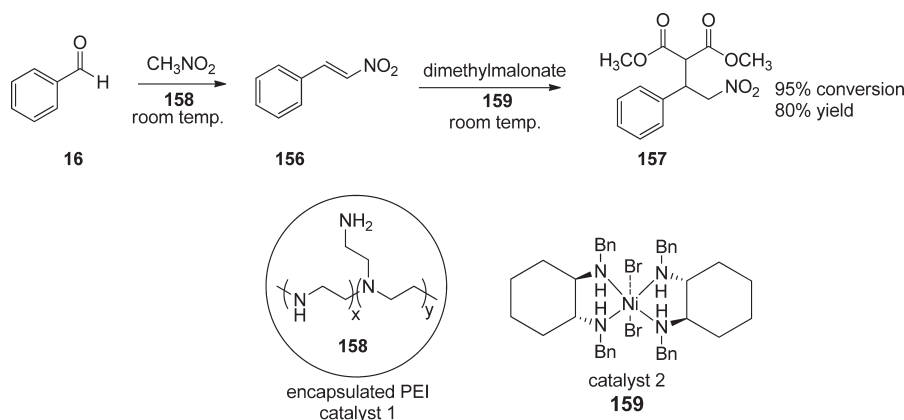
Other PEI derivatives have been used to catalyze a variety of reactions. For example, covalently linked microcapsules formed from PEI (compound **158**)¹⁶⁴ catalyzed the Knoevenagel condensation of benzaldehyde **16** and nitromethane to generate nitroalkene **156** (Scheme 9).¹⁶⁵ This initial product was reacted with nickel catalyst **159**¹⁶⁶ and dimethyl malonate to yield compound **157**. The covalent microcapsules successfully isolated the Lewis basic PEI from the Lewis acidic nickel catalyst and allowed the sequential reactions to occur in the same reaction vessel: the target product was formed in 80% yield (compared with 5% using free PEI and the nickel catalyst).

Frechet and co-workers reported that PEI could control the reaction pathway of enolizable aldehydes.¹⁶⁷ In the presence of a small-molecule proline catalyst,¹⁶⁸ enolizable aldehydes (**160**) can undergo either a reversible self-aldol condensation or an irreversible Mannich-type reaction that leads to formation of α,β -unsaturated aldehyde **161** (Scheme 10). The addition of modified hyperbranched PEI suppressed the irreversible reaction pathway, leading to the formation of the aldol product **162** in high yields and selectivities. PEI likely exercises control by

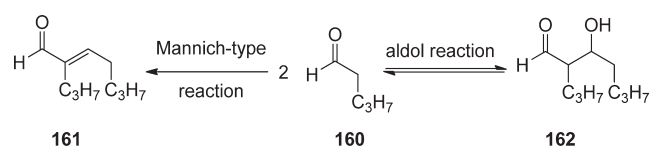
Table 5. Other Organic Reactions Catalyzed by PEI

Racemization of amino acids:	<p>43 + 42 $\xrightarrow{\text{pH 9.0, room temp}}$ ent-43 R = Me, Bn</p>
Decarboxylation of amino acids:	<p>154 + 42 $\xrightarrow{\text{pH 7.5, 60 }^\circ\text{C}}$ 155 + CO₂</p>

Scheme 9. Tandem Reaction Catalysis Using Encapsulated PEI



Scheme 10. Competing Reaction Pathways for Enolizable Aldehydes



imposing a hydrophobic environment, which in turn disfavors the Mannich-type reaction pathway that proceeds via a charged intermediate.

VII. MOLECULARLY IMPRINTED POLYMERS

VIIa. Introduction. Unlike PEI-based enzyme mimics, enzymes contain well-defined active sites. Another class of biomimetic catalysts, molecularly imprinted polymers (MIPs), have been synthesized with well-defined active sites that more closely mimic certain features of enzymatic active sites.^{169,170} These MIPs are designed to mimic certain key features of enzymes that contribute to their high catalytic activity. In particular,

- (1) enzymatic active sites are complementary in size and charge distribution to the target substrates;¹⁷¹
- (2) the active sites also contain catalytically active groups that participate in the reaction mechanism; and

- (3) the active sites bind the substrate through a variety of binding interactions, including electrostatic, hydrophobic, and hydrogen bonding attractive forces.

MIPs mimic these features by using an “imprinting strategy” to create a well-defined active site.¹⁷² Briefly, polymerizable groups are attached to a template molecule, which is copolymerized with a large excess of cross-linking agent in the presence of an inert solvent. Careful removal of the template yields a highly porous polymer with well-defined cavities that act as artificial active sites.

VIIb. Catalysis. An early example of such imprinting is shown in Figure 18.^{173,174} In this case, phenyl- α -D-mannopyranoside (the template) was covalently linked to two molecules of 4-vinylbenzene boronic acid (polymerizable groups) to yield compound **163**. After polymerization with ethylenedimethylacrylate and careful removal of the template, a MIP was formed. This MIP contained chiral cavities that were complementary in size and shape to phenyl- α -D-mannopyranoside. These cavities bound the D enantiomer substantially better than the mismatched L enantiomer (α values between 3.5 and 6.0).

The chiral cavities formed in MIPs have been used as chiral microreactors for asymmetric organic synthesis.¹⁷⁵ The first such example utilized chiral monomer **164** as a template.¹⁷⁶ After polymerization, the boronate and Schiff base linkages were hydrolyzed to yield a chiral cavity. Alkylation of glycine (compound **43c**)

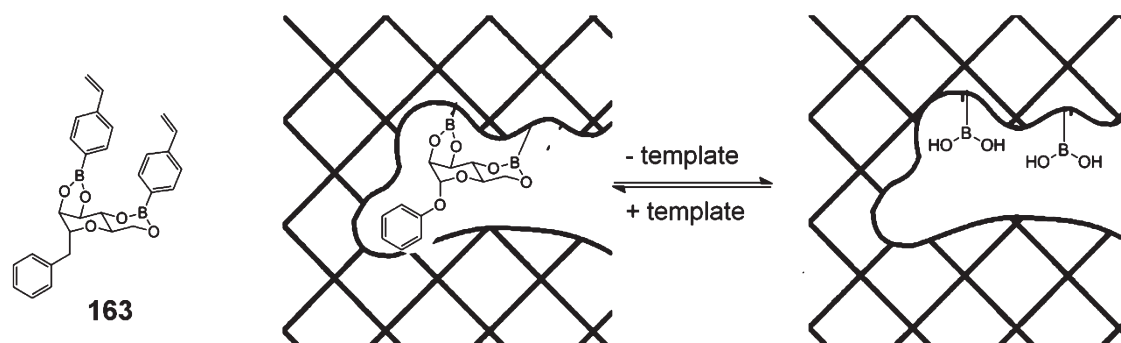
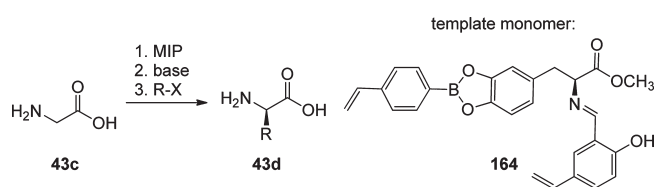


Figure 18. Early example of molecular imprinting to create a chiral cavity.

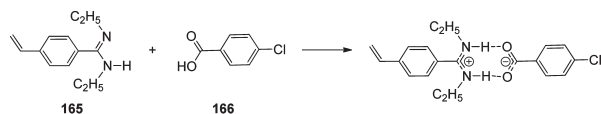
occurred inside these cavities to yield products (**43d**) with up to 36% ee (eq 20).



Equation 20: Asymmetric alkylation of glycine **43c** using an MIP

In addition to covalent linkages (i.e., Schiff bases¹⁷⁷ and boronate esters¹⁷⁸) that bind the template to the porous polymer structure, noncovalent linkages have also been used. These interactions, which include electrostatic¹⁷⁹ and hydrogen bonding¹⁸⁰ attractive forces, facilitate easy removal of the template. Single-point noncovalent interactions, however, are often not sufficiently selective.

In contrast, multi-point noncovalent interactions can bind the template in the polymer to form well-defined active sites. For example, amidine-containing template **165** forms a two-point hydrogen bond with carboxylic acids (i.e., *para*-chlorobenzoic acid, compound **166**) (eq 21).^{181,182} Following the removal of the template, these MIPs were used to bind carboxylic acid groups with high affinities.¹⁸³



Equation 21: Two-point hydrogen bond between amidine **165** and *para*-chlorobenzoic acid **166**

Catalytically active MIPs have also been synthesized using amidine templates. These MIPs often use a small molecule that mimics the putative transition state. Following polymerization, the template is removed to yield cavities that bind the transition state of the reaction better than either the starting material or the product. The high transition state affinity facilitates efficient catalytic turnover.

For example, amidine monomer **168** formed a two-point hydrogen bond with compound **167** (Figure 19).¹⁸⁴ This complex was polymerized in the presence of excess ethylenedimethacrylate. Following polymerization, compound **167** was removed by washing with a 0.1 M solution of sodium methoxide in methanol, which disrupts the hydrogen bonds. The resulting amidine-containing MIP catalyzed the hydrolysis of ester **169**,

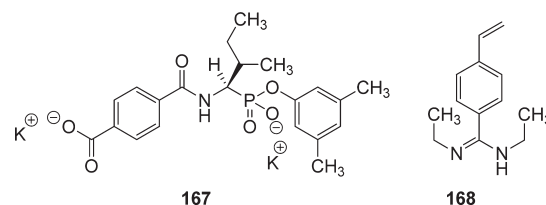
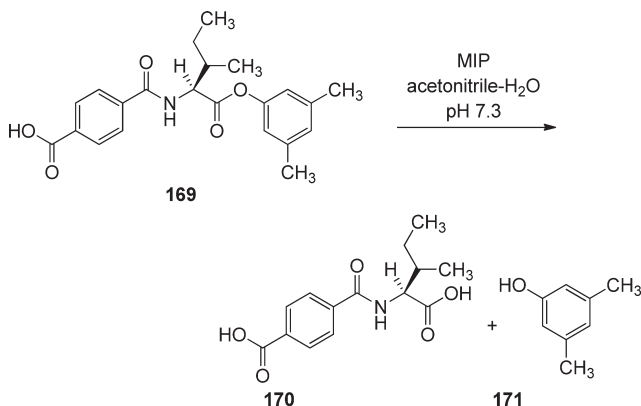


Figure 19. Transition state analogue **167** and functional monomer **168** used in MIP synthesis.

which proceeded 80 times faster in the presence of the MIP compared to the reaction in the presence of a control polymer (eq 22).

In addition, the cavities of the MIP act as chiral microreactors, with the hydrolysis of *L*-**169** proceeding 1.39 times faster than the hydrolysis of *D*-**169**. This chiral selectivity is determined by the chirality of the template **167** that was used to imprint the cavity.



Equation 22: Hydrolysis of ester **169** catalyzed by a MIP

Similarly, Nicholls and co-workers designed a MIP that mimics the enzyme transaminase.¹⁸⁵ This MIP used compound **173** to mimic the putative reaction transition state (Figure 20). (A detailed mechanism of transamination is discussed in the previous section of this review.) Compound **173** was copolymerized with a large excess of cross-linker, followed by removal of the template.¹⁸⁶

The resulting MIP catalyzed the transamination of phenylpyruvic acid to phenylalanine with a 15-fold rate acceleration (compared with the polymer-free reaction) (eq 23). Furthermore, the product phenylalanine was produced in 32% L ee, as a result of the chiral environment in the MIP's active sites. Other

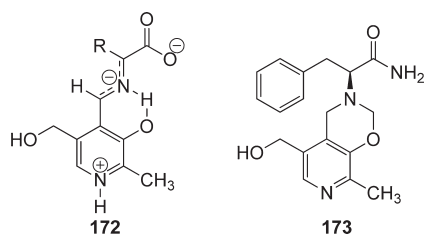
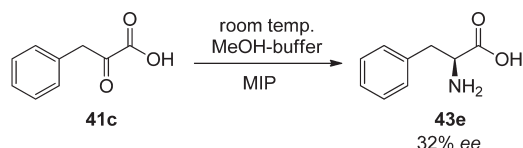


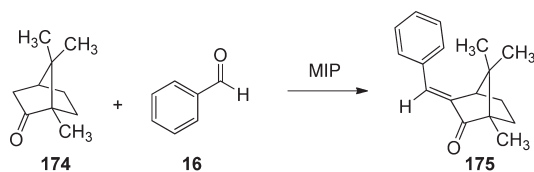
Figure 20. Proposed transition state of the transamination reaction (172) and a covalent transition state analogue used for MIP synthesis (173).

catalytically active^{187,188} and enantioselective MIPs have also been reported.



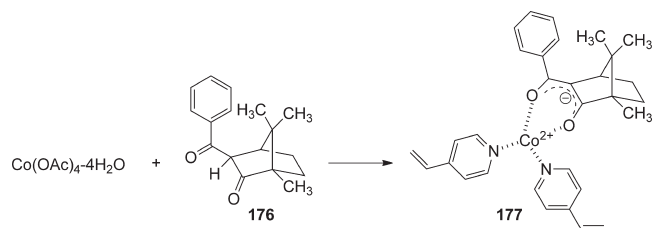
Equation 23: Synthesis of phenylalanine from phenylpyruvic acid using a MIP

MIPs have also been used to catalyze a variety of carbon–carbon bond-forming reactions. For example, Mosbach and co-workers reported that a MIP catalyzed the aldol reaction of camphor **174** and benzaldehyde **16** with a 55-fold rate enhancement compared with the polymer-free reaction (eq 24).¹⁸⁹



Equation 24: Aldol reaction catalyzed by an MIP

The MIP was synthesized by mixing diketone template **176** and $\text{Co}(\text{OAc})_4 \cdot 4\text{H}_2\text{O}$ with 4-vinylpyridine, styrene, divinylbenzene, and a radical initiator. Cobalt likely forms coordination complex **177** (eq 25), with two of its binding sites occupied by the diketone carbonyls. This metal–ligand complex forces the diketone to adopt a planar geometry, which closely mimics the geometry of the reaction transition state.



Equation 25: Putative metal-ligand complex **177** used as a transition state mimic template

An earlier report by the same research group found that a MIP catalyzed a different aldol condensation with an 8-fold enhancement in the reaction rate.¹⁹⁰ MIP-based catalysis of

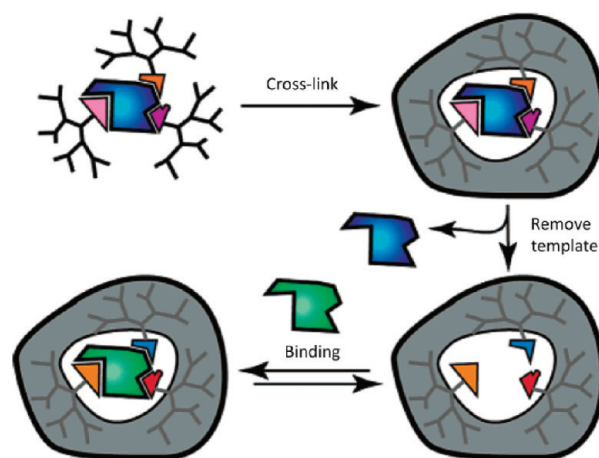


Figure 21. Design of a MIP dendrimer with a single active site (reprinted from ref 193).

cycloadditions, such as the Diels–Alder reaction¹⁹¹ and the Huisgen cycloaddition,¹⁹² has also been reported.

One drawback in the design of catalytic MIPs is that multiple catalytic sites are generated from the small-molecule template. The somewhat unpredictable environment of each active site may diminish the catalytic efficiency of these systems. To circumvent this problem, Zimmerman and co-workers designed a molecularly imprinted dendrimer that contained a single active site.¹⁹³ A schematic illustration of Zimmerman's work is shown in Figure 21. The dendrimer is first cross-linked to create a covalently bound, well-defined periphery from which the template is later removed.

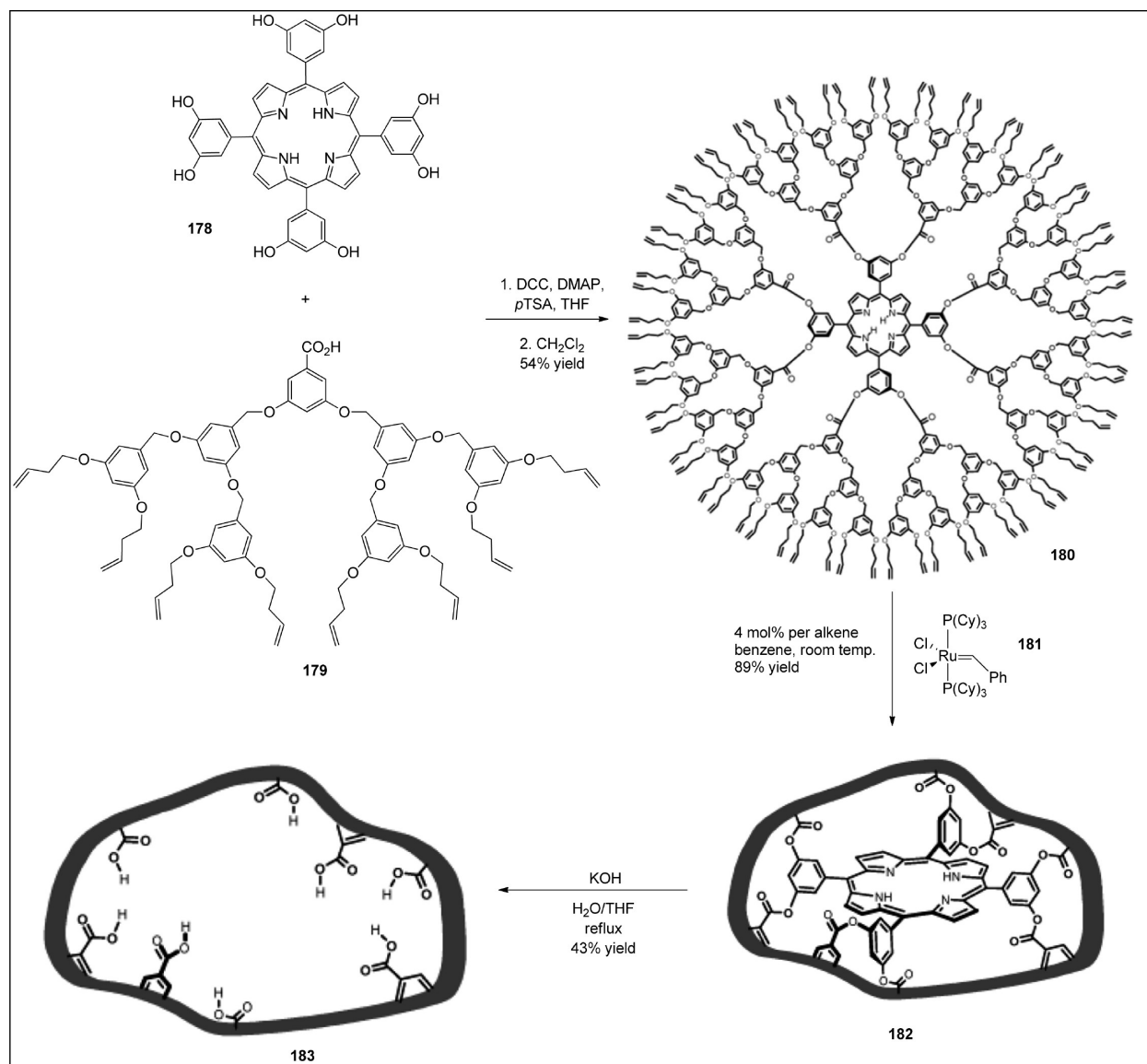
Specifically, hydroxyphenyl porphyrin **178** was used as the template (Scheme 11). Following esterification with carboxylic acid **179**, the dendrimer periphery was treated with Grubbs' catalyst under high dilution conditions to yield covalently linked dendrimer **182**. Although calculations indicate that numerous potential isomers could be formed from the cross-linking reaction, only a small subset of such isomers was detected by ¹H NMR. After completion of the metathesis reaction, removal of the porphyrin template under basic conditions generated a monomolecular porphyrin-imprinted dendrimer **183**. The resulting imprinted dendrimer showed moderately strong binding affinities for a variety of porphyrin guests.

VIII. ORGANOCATALYSIS

VIIIa. Introduction. In the previous sections of this review, large-molecule enzyme mimics were discussed in some detail. These compounds have been moderately successful in mimicking certain enzymatic features, such as the formation of artificial active sites with an environment that differs from that of the bulk medium. More recently, organic chemists have utilized smaller molecules to mimic key features of enzymatic catalysis.^{194–196} This active research area of organocatalysis can trace many of its origins to the older field of biomimetic catalysis.

For example, enzymes stabilize the reactant transition state through a variety of noncovalent interactions. Biomimetic catalysts such as MIPs have successfully mimicked this feature. Similarly, small-molecule organocatalysts, including oligopeptides¹⁹⁷ (Scott Miller) and thioureas¹⁹⁸ (Eric Jacobsen) utilize noncovalent interactions. Another class of organocatalysts is secondary

Scheme 11. Synthesis of a Porphyrin-Imprinted Dendrimer



amines,¹⁹⁹ which have been used to mimic a variety of enzymes. These catalysts generally effect rate accelerations through a combination of iminium²⁰⁰ and enamine activation.²⁰¹ Finally, *N*-heterocyclic carbenes (NHCs) catalyze a variety of organic reactions. Their widespread success has been inspired by the natural thiamine cofactor, which is used to accelerate the benzoin condensation (as well as other reactions).

In the final section of this review article, we will discuss the connection between biomimetic catalysis and organocatalysis and highlight several notable examples.

VIIIb. Noncovalent Organocatalysis. Although many biomimetic catalysts use hydrophobic binding as a noncovalent interaction to achieve efficient catalysis, other noncovalent interactions (such as hydrogen bonding or electrostatic interactions) have been less developed.

Scott Miller and co-workers developed a series of oligopeptides that utilize noncovalent interactions to achieve catalysis.²⁰² One notable example is shown in eq 26.^{203,204} The ultimate goal

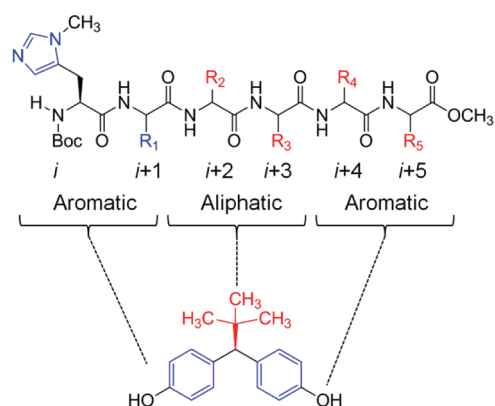


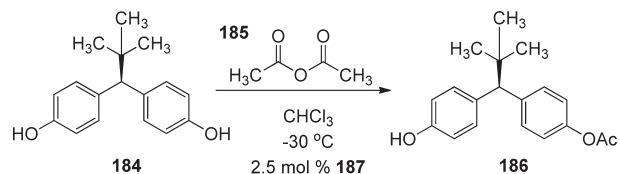
Figure 22. Schematic illustration of rational peptide catalyst design.

was to achieve the efficient desymmetrization of prochiral bisphenol **184** via acylation. Using enzymatic catalysis, only 40%

Table 6. Organic Reactions Catalyzed by Miller's Oligopeptides

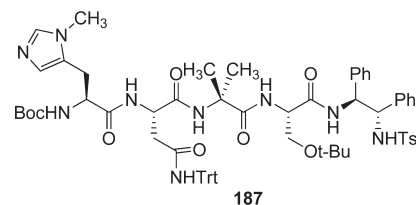
Reaction #	Reaction name	Reaction structure	Catalyst structure
Reaction 1	Phosphorylation	<p>188</p> <p>189 65% yield >98% ee</p>	<p>190</p>
Reaction 2	Azide addition	<p>191</p> <p>192 95% yield</p>	<p>193</p> <p>Xaa = L-phe</p>
Reaction 3	Dynamic kinetic resolution	<p>194</p> <p>195 90% yield 92:8 enantiomeric ratio</p>	<p>196</p> <p>H₃C-N(CH₃)₂</p>

yield (with 99% ee after recrystallization) was achieved. This substrate is particularly challenging because the two phenols are separated by nearly a full nanometer and are ~ 5.7 Å removed from the prochiral *tert*-butyl center.

Equation 26: Peptide-catalyzed desymmetrization of bisphenol **184**

An initial library of hexapeptides was screened, with each peptide containing a general aromatic–aliphatic–aromatic motif (Figure 22) designed to bind to particular elements of the substrate. After several rounds of optimization, a highly efficient tetrapeptide (compound **187**) was identified as the optimal catalyst, affording the desired monoacylated product in 80% yield and 95% ee. Mechanistic studies suggested that the phenolic OH may interact with the catalyst via hydrogen bonding, and the phenyl rings interact with the catalyst as well. This multi-point noncovalent attraction enables such efficient catalysis, which surpasses that of enzymatic catalysis.

Other reactions catalyzed by Miller's oligopeptides are shown in Table 6 and include the asymmetric phosphorylation of cyclic triols,²⁰⁵ the conjugate addition of azides to unsaturated carbonyls,²⁰⁶ and the dynamic kinetic resolution of biaryl atropisomers.²⁰⁷ In all cases, mechanistic investigations indicate

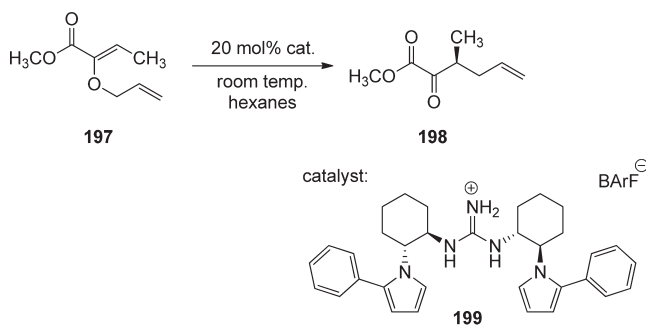
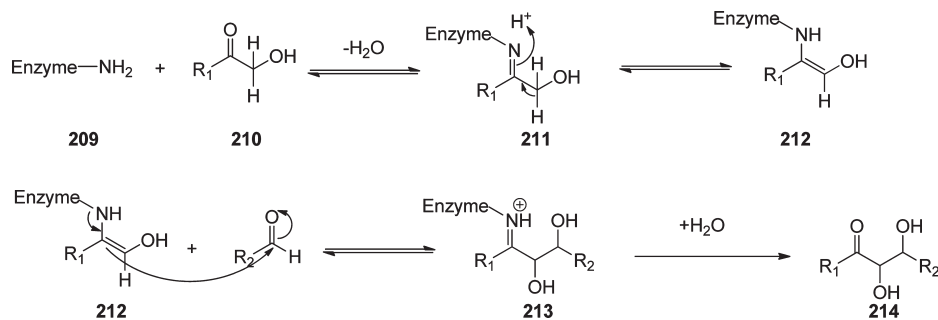


that the catalyst likely interacts with the substrate via multiple noncovalent interactions, which are responsible for the high levels of enantioselectivity observed.

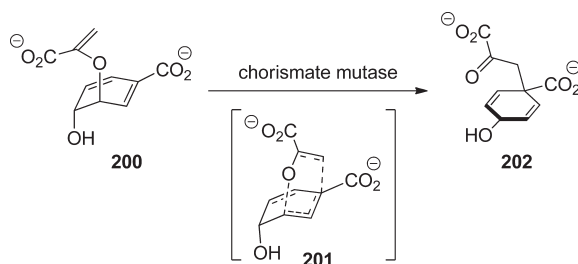
Similarly, Jacobsen and co-workers have developed chiral hydrogen-bonding catalysts that use noncovalent interactions to achieve high levels of enantioinduction. For example, the Claisen rearrangement of substrate **197** in the presence of 20 mol % of catalyst **199** afforded compound **198** in high yield and enantioselectivity (eq 27).^{208,209}

This reaction mimics the enzyme chorismate mutase, which utilizes noncovalent interactions to stabilize the charged transition state (compound **201**) in the Claisen rearrangement of compounds **200** to **202** (eq 28). Up to 10^6 -fold rate accelerations are observed for this enzymatic reaction. Similarly, catalyst **199** catalyzes the Claisen rearrangement using a combination of cation– π and hydrogen bonding interactions.

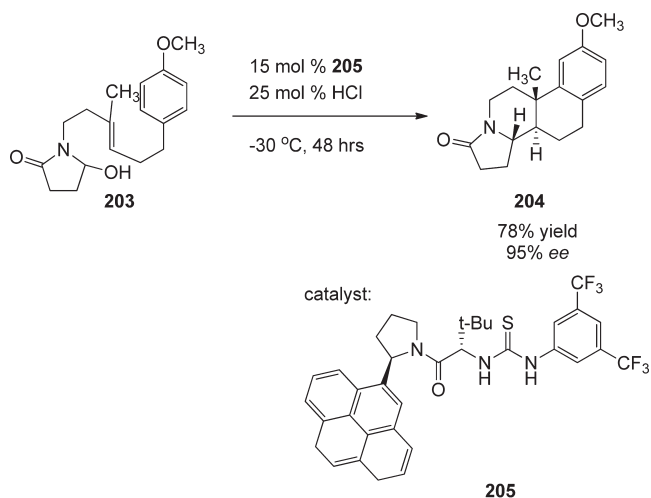
The cationic polycyclization of compound **203** was also accelerated by hydrogen-bonding thiourea catalyst **205** (eq 29).²¹⁰ The large aromatic pyrene substituent of the catalyst was necessary to achieve high yields and ee's, which indicates that cation– π interactions are operative in this system.

Scheme 12. Mechanism of an Aldolase Class I Enzyme with Hydroxy Acid Starting Material **210**

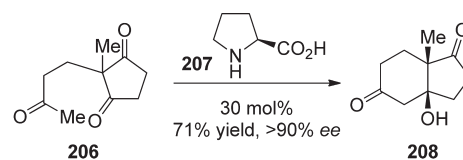
Equation 27: Guanidium-catalyzed Claisen rearrangement



Equation 28: Enzyme-catalyzed Claisen rearrangement

Equation 29: Cationic polycyclization catalyzed by chiral thiourea **205**

VIIIc. Secondary Amine Catalysis. Secondary amines, in particular, proline and proline-based derivatives, have been used to catalyze a wide variety of reactions.²¹¹ The first intramolecular aldol reaction catalyzed by a secondary amine was reported concurrently by Hajos-Parish²¹² and Wiechert²¹³ in 1974 (eq 30).

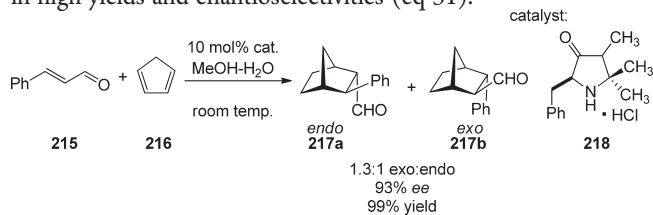


Equation 30: Original Hajos-Wiechert reaction, reported in 1974

This reaction mimics the enzymatic activity of class I aldolases, which catalyze aldol reactions via formation of an iminium intermediate.²¹⁴ The iminium (compound **211**) is subsequently converted into an enzyme-bound enamine nucleophile (**212**) that attacks an aldehyde electrophile (Scheme 12). Hydrolysis of the imine forms the desired aldol product (**214**). This enzymatic mechanism, which was first proposed in 1964,²¹⁵ has been proven correct through subsequent experimentation.²¹⁶

Although the proline-catalyzed aldol reaction likely occurs via a mechanism similar to that of class I aldolases, its precise mechanism has been debated. The generally accepted mechanism is that a single proline molecule catalyzes the reaction via formation of an enamine intermediate that attacks the aldehyde. In addition, general acid catalysis (using the carboxylic acid of the proline) activates the aldehyde for attack by the enamine. This mechanism is supported by computational^{217,218} and mechanistic studies.²¹⁹

Following the initial reports of Hajos and Wiechert, 26 years passed until the next report that used secondary amines as organocatalysts. In 2000, David MacMillan and co-workers reported that a chiral imidazolidinone catalyzed the Diels–Alder reaction of *trans*-cinnamaldehyde **215** and cyclopentadiene **216** in high yields and enantioselectivities (eq 31).²²⁰

Equation 31: Enantioselective Diels-Alder reaction catalyzed by chiral imidazolidinone **218**

Scheme 13. Proposed Catalytic Cycle for the Imidazolidinone-Catalyzed Diels-Alder Reaction

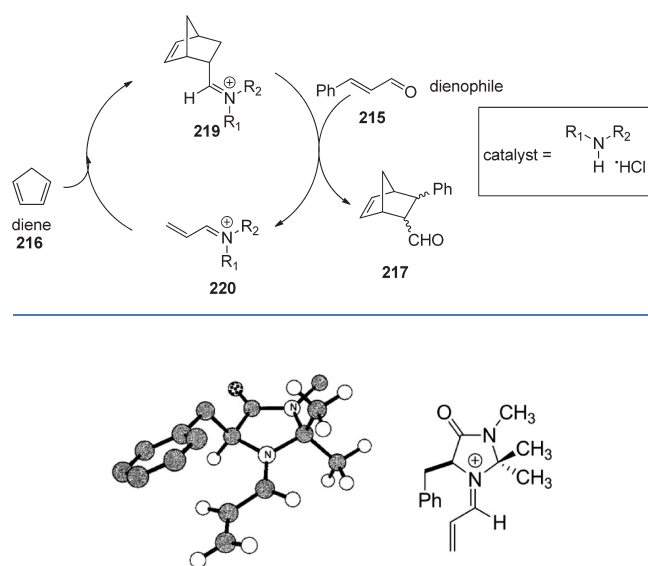
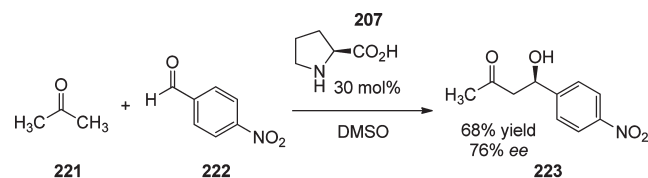


Figure 23. Energy-minimized structure of sterically bulky iminium intermediate.

The proposed catalytic cycle is shown in Scheme 13 and involves the formation of a transient iminium ion that lowers the LUMO of the dienophile. This reaction is related to early work on the asymmetric Diels–Alder reaction of chiral iminium salts.²²¹ The major advance of MacMillan's work is that he was able to achieve efficient catalysis.

The high *ee*'s in this Diels–Alder reaction are likely due to the bulky iminium group, which successfully blocks one side of the dienophile (Figure 23).

In the same year as MacMillan's initial report, List, Lerner, and Barbas reported the first asymmetric intermolecular aldol reaction catalyzed by proline (eq 32).²²² The proposed mechanism involves formation of an enamine intermediate and is similar to the Hajos–Wiechert mechanism.



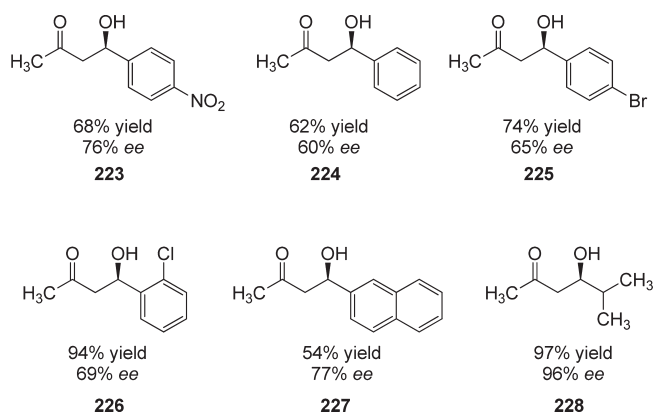
Equation 32: Initial report of an asymmetric intermolecular aldol reaction

A wide variety of substrates were subjected to this aldol reaction, and the products were formed in up to 97% yield and up to 96% *ee* (Chart 6).

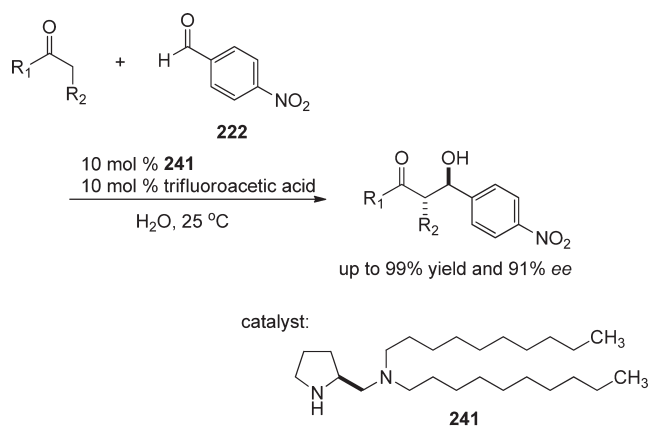
Following these initial papers on secondary amine catalysis, many other amine-catalyzed reactions were reported. For example, MacMillan used a slightly modified imidazolidinone catalyst **232** to achieve the enantioselective coupling of a variety of substituted indoles with α,β -unsaturated aldehydes.²²³ Other examples of reactions catalyzed by chiral imidazolidinones are shown in Table 7.^{224–226}

The field of enamine catalysis, meaning the catalytic activation of carbonyl compounds via enamine intermediates, has also

Chart 6. Products of the proline-catalyzed asymmetric aldol reaction



expanded greatly.^{168,227} The discussion here will focus on the connection between enamine organocatalysis and biomimetic chemistry. In particular, Barbas and co-workers have developed a series of reactions that successfully mimic class I aldolase enzymes. For example, compound **241** efficiently catalyzed the aldol reaction of a variety of aldehyde and ketone donors with aryl aldehyde acceptors (such as compound **222**) (eq 33).²²⁸ This broad substrate scope mimics the enzyme deoxyribose-5-phosphate (DERA) aldolase,²²⁹ which is likewise able to accommodate multiple substrates. Moreover, the long alkyl chains of **241** bind to and sequester the organic substrate, which allows the reaction to proceed in aqueous media. Prior to the development of this organocatalytic reaction, Barbas used DERA aldolase itself as a synthetic catalyst.²³⁰



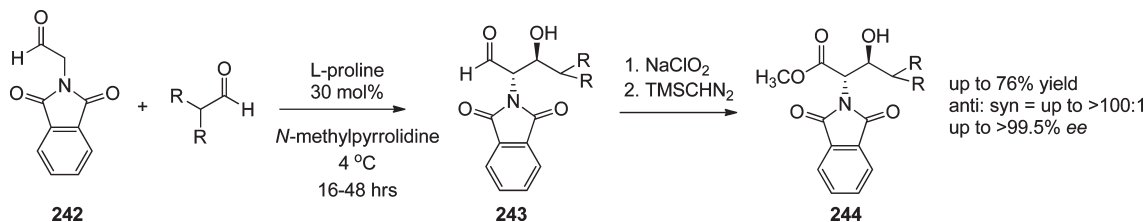
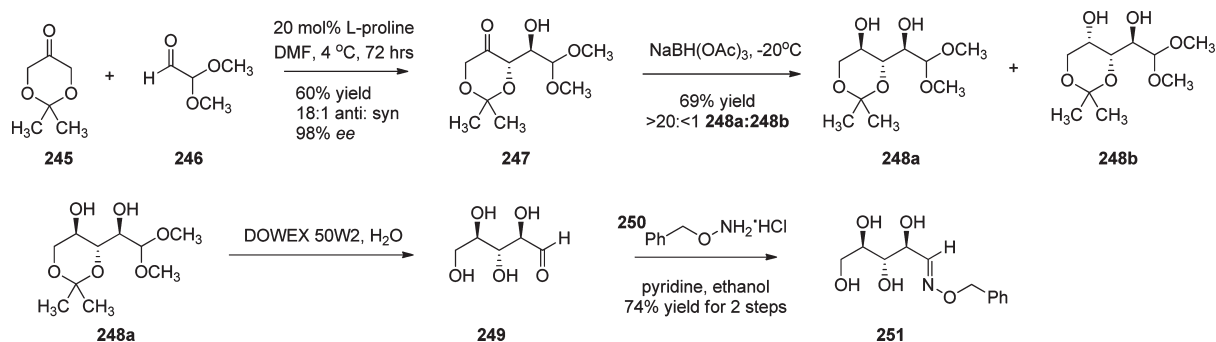
Equation 33: Organocatalytic reaction that mimics DERA aldolase

L-Proline (**207**) can also catalyze the formation of β -hydroxy- α -amino acids via an asymmetric aldol reaction (Scheme 14),²³¹ which mimics the natural enzyme threonine aldolase.²³² The initial aldehyde products **243** can be converted to amino esters **244** via straightforward chemical manipulation.

The enantioselective de novo synthesis of carbohydrates can be achieved using an asymmetric aldol reaction as the key step.²³³ Specifically, protected dihydroxyacetone **245** and aldehyde **246** underwent a proline-catalyzed aldol reaction to generate compound **247** in moderate yield and excellent diastereo- and enantioselectivity (Scheme 15). This compound was reacted further to afford D-ribose

Table 7. Sample Reactions Catalyzed by Chiral Imidazolidinone **232**

Reaction:	Catalyst:	Counter-ion
Reaction 1: Conjugate addition of indole 	 232	 233
Reaction 2: Conjugate amine addition 	 232	 236
Reaction 3: Mukaiyama- Michael reaction 	 232	 239
Reaction 4: Aldehyde- aldehyde coupling 	 232	 233

Scheme 14. Organocatalytic Synthesis of β -Hydroxy- α -amino EstersScheme 15. De Novo Synthesis of D-Ribose (compound **249**) Using Asymmetric Organocatalysis

(compound **249**), which was isolated as the corresponding oxime **251** in 31% overall yield over four steps. Other carbohydrates, including L-ribulose, L-lyxose, and D-tagatose, were also synthesized via this method. These synthetic sequences

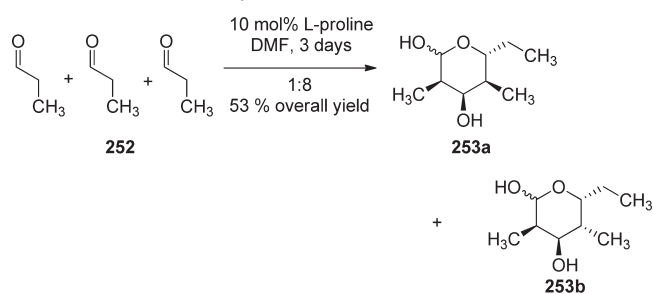
successfully mimic the enzymes tagatase aldolase and fucose aldolase.²³⁴

The self-aldol trimerization of propionaldehyde **252** can likewise be catalyzed by proline to yield the corresponding pyranose

Table 8. Other Examples of Organocatalysis by Proline-Based Compounds

Reaction 1:	Mannich reaction		
Reaction 2:	aldehyde alkynylation		
Reaction 3:	α -aminoxylation		

carbohydrates in high yields and selectivities (eq 34).²³⁵ Other examples of aldol reactions catalyzed by secondary amines are summarized in a variety of review articles.^{196,236,237}



Equation 34: Proline-catalyzed trimerization of propionaldehyde

Other reactions catalyzed by proline and proline derivatives are summarized in Table 8 and include a variety of Mannich reactions^{238–241} as well as aldehyde alkynylation²⁴² and α -aminoxylation.^{243–246}

Blackmond and co-workers studied the mechanism of the proline-catalyzed α -aminoxylation (Table 8, reaction 3)²⁴⁷ and found that both the reaction rate and the product enantiomeric excess increased throughout the course of the reaction. These unusual observations suggest that an autocatalytic mechanism is operative, wherein the product itself catalyzes the formation of more chiral product.²⁴⁸ To support this hypothesis, non-enantiopure proline was used as the catalyst, and the resulting product ee's were higher than what would be expected on the basis of a linear relationship (Figure 24).

Mechanistic models to explain autocatalytic reactions have been proposed by Kagan²⁴⁹ and others.^{250,251} These reactions have potential implications for the origin of biomolecular homochirality, which requires a prebiotically feasible mechanism of enantiomeric amplification.^{252–254}

VIIId. N-Heterocyclic Carbene (NHC) Catalysis. PEI, in combination with a thiamine-derived cofactor, catalyzes the benzoin

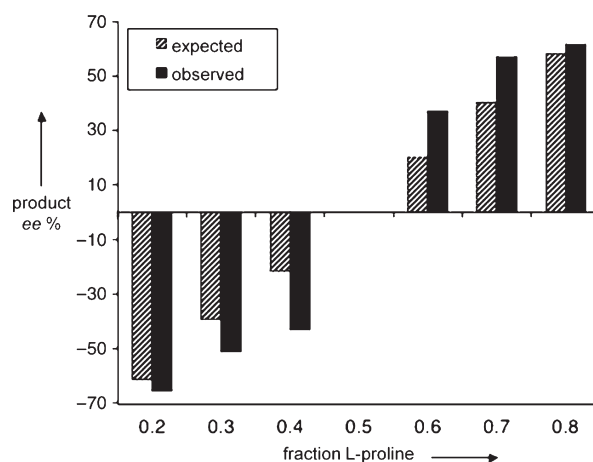
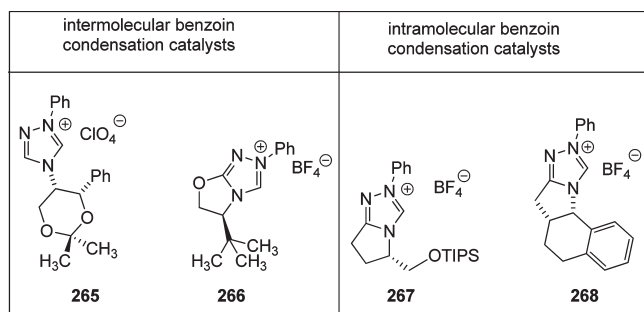


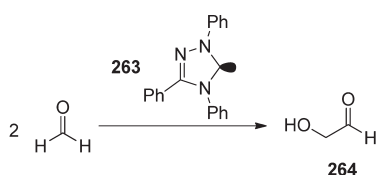
Figure 24. Final product ee as a function of the proline catalyst ee for the α -aminoxylation of aldehydes.

condensation reaction (vide infra).¹⁶² The thiamine cofactor converts the normally electrophilic aldehyde into a nucleophilic, acyl anion equivalent. This reaction effectively mimics transketolase enzymes,²⁵⁵ which catalyze the addition of 2-carbon “active aldehyde” units using a thiamine cofactor. Mechanistically, the thiamine cofactor is converted into a carbene, which in turn attacks the aldehyde to generate a neutral complex known as the “Breslow intermediate.”¹⁶³ This intermediate then acts as a nucleophile and attacks a second carbonyl to accomplish the key C–C bond formation. Release of the product regenerates the catalytically active carbene (Scheme 8).

The field of organocatalysis has achieved significant success using bioinspired NHC catalysis. NHCs, like thiamine, catalyze organic reactions by converting a normally electrophilic aldehyde into a nucleophilic “acyl anion” equivalent. An early example of NHC catalysis was reported by Enders and co-workers, who utilized triazole-derived carbene **263** to catalyze the benzoin-like condensation of formaldehyde (eq 35).^{256,257} Moreover, asymmetric inter- and intramolecular benzoin

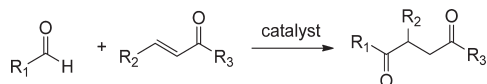
Chart 7. Chiral Carbenes Used for the Asymmetric Benzoin Condensation

condensations have been catalyzed by chiral NHC catalysts (Chart 7).^{258–261}



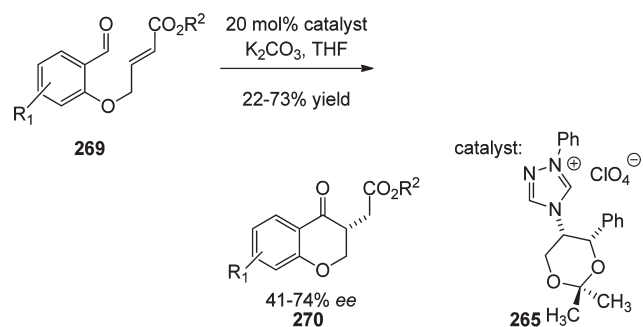
Equation 35: NHC-catalyzed benzoin-type condensation of formaldehyde

In addition to the benzoin condensation, the Stetter reaction can also be catalyzed by NHCs. In general, the Stetter reaction involves the conjugate addition of a nucleophilic aldehyde equivalent to an α,β -unsaturated ketone to generate 1,4-diketone products (eq 36). Achiral Stetter reactions are typically catalyzed by cyanide anions or achiral thiazolium salts.



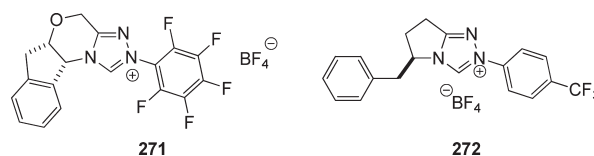
Equation 36: General depiction of the Stetter reaction

In 1996, Enders reported the first NHC-catalyzed asymmetric Stetter reaction (eq 37), which produced chiral chromanones **270** in moderate yields and ee's.²⁶² Following this initial report, several chiral thiazolium-derived carbenes were used as asymmetric catalysts for the Stetter reaction,^{263,264} although modest ee's were often obtained.²⁶⁵



Equation 37: Asymmetric intra-molecular Stetter reaction

One notable exception was reported by Tomislav Rovis and co-workers, who synthesized carbenes **271** and **272** (Chart 8).

Chart 8. N-Heterocyclic Carbenes Used for Highly Enantioselective Stetter Reaction

With only 3 mol % catalyst loading, the desired products could still be formed in up to 97% yield and 99% ee.²⁶⁶ The general mechanism of the NHC-catalyzed Stetter reaction is similar to that of the benzoin condensation, that is, initial attack by the carbene generates a nucleophilic aldehyde species. However, DFT calculations indicate that there may be some subtle mechanistic differences.²⁶⁷

There are many other subtopics in organocatalysis, including organocatalysis in cascade reactions^{268–270} and the use of organocatalysis in the total synthesis of complex molecules.^{271,272} This section has focused only on the connections between organocatalysis and biomimetic catalysis.

IX. CONCLUSION

Over the past 40 years, chemists have made significant advances in designing and synthesizing enzyme mimics, which effectively imitate several features of enzymes that facilitate efficient catalysis. In turn, these mimics have been used to catalyze a wide variety of organic reactions, including the transamination reaction of ketoacids to amino acids, the Diels–Alder cycloaddition of a variety of dienes and dienophiles, and the acylation and phosphorylation of alcohols. In some of these cases, the biomimetic catalysts have surpassed the rate accelerations and regioselectivities of the natural enzymes.

Some notable examples include the 10¹²-fold rate acceleration reported by Irving Klotz in the hydrolysis of 2-hydroxy-5-nitrophenylsulfate to 4-nitrocatechol, and the 725 000-fold rate acceleration for the transamination of indolepyruvic acid to tryptophan reported by Breslow and co-workers. The highly active field of organocatalysis has utilized many of the key reactions and mechanistic understandings achieved by biomimetic chemists to develop a new(er) research field.

As society becomes increasingly aware of the negative influences that an industrialized community has on the environment, the field of biomimetic chemistry offers a considerable number of solutions. By understanding nature's synthetic processes, we can begin to draw inspiration based on observation and dramatically cut down on the amount of hazardous material utilized within the research setting. In most cases, biomimetic chemistry offers an environmentally friendly approach to synthesis due in large part to the catalyst's ability to carry out complex reactions in water, as opposed to the more toxic solvents that often are over-relied-upon in the laboratory. Furthermore, the field of biomimetic chemistry presents investigators with a more cost-effective means of synthesis. Most catalysts have the ability to optimize reactions, allowing for higher yields and can often be recycled and re-used.

AUTHOR INFORMATION

Corresponding Author

*mlevine@chm.uri.edu.

ACKNOWLEDGMENT

We graciously acknowledge the chemistry department at the University of Rhode Island for providing generous funding. Ms. Nicole Cook is also thanked for her editorial suggestions and expertise.

REFERENCES

- Breslow, R. *J. Biol. Chem.* **2009**, *284*, 1337–1342.
- Breslow, R. *Chem. Soc. Rev.* **1972**, *1*, 553–580.
- Leete, E. *J. Chem. Soc. Chem. Commun.* **1972**, 1091.
- Burke, D. E.; Le Quesne, P. W. *J. Chem. Soc. Chem. Commun.* **1972**, 678.
- Breslow, R.; Dong, S. D. *Chem. Rev.* **1998**, *98*, 1997–2011.
- He, Q.; Cui, Y.; Li, J. *Chem. Soc. Rev.* **2009**, *38*, 2292–2303.
- Nicolaou, K. C.; Montagnon, T.; Snyder, S. A. *Chem. Commun.* **2003**, 551–564.
- Liu, L.; Zhou, W.; Chruma, J.; Breslow, R. *J. Am. Chem. Soc.* **2004**, *126*, 8136–8137.
- Spetnagel, W. J.; Klotz, I. M. *J. Am. Chem. Soc.* **1976**, *98*, 8199–8204.
- Decreau, R. A.; Collman, J. P.; Hosseini, A. *Chem. Soc. Rev.* **2010**, *39*, 1291–1301.
- Feig, A. L.; Lippard, S. J. *Chem. Rev.* **1994**, *94*, 759–805.
- Breslow, R. *Wiley Encyclopedia of Chemical Biology*; John Wiley & Sons: Hoboken, NJ, 2009; Vol. 3; pp 277–284
- Che, C.-M.; Huang, J.-S. *Chem. Commun.* **2009**, 3996–4015.
- Walsh, C. *Enzymatic Reaction Mechanisms*, 2nd ed.; W. H. Freeman and Company: New York, 1978.
- Kirby, A. J.; Hollfelder, F. *From Enzyme Models to Model Enzymes*; RSC Publishing: Cambridge, 2009.
- Silverman, R. B. *The Organic Chemistry of Enzyme-Catalyzed Reactions*, 2nd ed.; Academic Press: San Diego, 2002.
- Carter, P.; Wells, J. A. *Nature* **1988**, *332*, 564–568.
- Heinz, D. W. *Angew. Chem., Int. Ed.* **1999**, *38*, 2348–2351.
- Breslow, R. *J. Phys. Org. Chem.* **2006**, *19*, 813–822.
- Breslow, R.; Maitra, U.; Rideout, D. *Tetrahedron Lett.* **1983**, *24*, 1901–1904.
- Breslow, R.; Bandyopadhyay, S.; Levine, M.; Zhou, W. *Chem-BioChem* **2006**, *7*, 1491–1496.
- Alberts, B.; Johnson, A.; Lewis, J.; Raff, M.; Roberts, K.; Walter, P. *Molecular Biology of the Cell*, 5th ed.; Garland Science: New York, 2008; pp 159–174.
- Radzicka, A.; Wolfenden, R. *Science* **1995**, *267*, 90–93.
- McKee, T.; McKee, J. R. *Biochemistry: The Molecular Basis of Life*, 3rd ed.; McGraw-Hill: New York, 2003.
- Griffiths, D. W.; Bender, M. L. *Adv. Catal.* **1973**, *23*, 209–261.
- Akkilagunta, V. K.; Reddy, V. P.; Kakulapati, R. R. *Synlett* **2010**, 2571–2574.
- Singleton, M. L.; Reibenspies, J. H.; Darensbourg, M. Y. *J. Am. Chem. Soc.* **2010**, *132*, 8870–8871.
- Madhav, B.; Murthy, S. N.; Reddy, V. P.; Rao, K. R.; Nageswar, Y. V. D. *Tetrahedron Lett.* **2009**, *50*, 6025–6028.
- Wang, Q.; Yang, Z.; Zhang, X.; Xiao, X.; Chang, C. K.; Xu, B. *Angew. Chem., Int. Ed.* **2007**, *46*, 4285–4289.
- Marinescu, L.; Bols, M. *Curr. Org. Chem.* **2010**, *14*, 1380–1398.
- Bellia, F.; La Mendola, D.; Pedone, C.; Rizzarelli, E.; Saviano, M.; Vecchio, G. *Chem. Soc. Rev.* **2009**, *38*, 2756–2781.
- Bjerre, J.; Rousseau, C.; Marinescu, L.; Bols, M. *Appl. Microbiol. Biotechnol.* **2008**, *81*, 1–11.
- Bhosale, S. V.; Bhosale, S. V. *Mini-Rev. Org. Chem.* **2007**, *4*, 231–242.
- Barr, L.; Dumanski, P.; Easton, C.; Harper, J.; Lee, K.; Lincoln, S.; Meyer, A.; Simpson, J. *J. Inclusion Phenom. Macrocyclic Chem.* **2004**, *50*, 19–24.
- D'Souza, V. T. *Supramol. Chem.* **2003**, *15*, 221–229.
- Motherwell, W. B.; Bingham, M. J.; Six, Y. *Tetrahedron* **2001**, *57*, 4663–4686.
- Suzuki, I.; Miura, T.; Anzai, J.-I. *J. Supramol. Chem.* **2003**, *1*, 283–288.
- Menuel, S.; Corvis, Y.; Rogalska, E.; Marsura, A. *New J. Chem.* **2009**, *33*, 554–560.
- Liu, Y.; You, C.-C. *Chin. J. Chem.* **2001**, *19*, 533–544.
- Rideout, D. C.; Breslow, R. *J. Am. Chem. Soc.* **1980**, *102*, 7816–7817.
- Das, T.; Kumar, A.; Ghosh, P.; Maity, A.; Jaffer, S. S.; Purkayastha, P. *J. Phys. Chem. C* **2010**, *114*, 19635–19640.
- Isaacs, L. *Chem. Commun.* **2009**, 619–629.
- Kim, K.; Selvapalam, N.; Ko, Y. H.; Park, K. M.; Kim, D.; Kim, J. *Chem. Soc. Rev.* **2007**, *36*, 267–279.
- Lagona, J.; Mukhopadhyay, P.; Chakrabarti, S.; Isaacs, L. *Angew. Chem., Int. Ed.* **2005**, *44*, 4844–4870.
- Rebek, J. *Acc. Chem. Res.* **2009**, *42*, 1660–1668.
- Pluth, M. D.; Bergman, R. G.; Raymond, K. N. *Acc. Chem. Res.* **2009**, *42*, 1650–1659.
- Breslow, R.; Kohn, H.; Siegel, B. *Tetrahedron Lett.* **1976**, 1645–1646.
- Breslow, R.; Campbell, P. *J. Am. Chem. Soc.* **1969**, *91*, 3085.
- Breslow, R.; Campbell, P. *Bioorg. Chem.* **1971**, *1*, 140–156.
- Hennrich, N.; Cramer, F. *J. Am. Chem. Soc.* **1965**, *87*, 1121–1126.
- VanEtten, R. L.; Sebastian, J. F.; Clowes, G. A.; Bender, M. L. *J. Am. Chem. Soc.* **1967**, *89*, 3242–3253.
- VanEtten, R. L.; Clowes, G. A.; Sebastian, J. F.; Bender, M. L. *J. Am. Chem. Soc.* **1967**, *89*, 3253–3262.
- Brown, F. S.; Hager, L. P. *J. Am. Chem. Soc.* **1967**, *89*, 719–720.
- Szejtli, J. *Cyclodextrins and Their Inclusion Complexes*; Akademiai Kiado: Hungary, 1982.
- Dodziu, K. H. *Cyclodextrins and Their Complexes: Chemistry, Analytical Methods, Applications*. Wiley-VCH: Weinheim, 2006.
- Schneider, H. J.; Sangwan, N. K. *J. Chem. Soc. Chem. Commun.* **1986**, 1787–1789.
- Chung, W.-S.; Wang, J.-Y. *J. Chem. Soc. Chem. Commun.* **1995**, 971–972.
- Murthy, S. N.; Madhav, B.; Kumar, A. V.; Rao, K. R.; Nageswar, Y. V. D. *Tetrahedron* **2009**, *65*, 5251–5256.
- Breslow, R.; Overman, L. E. *J. Am. Chem. Soc.* **1970**, *92*, 1075–1077.
- Bulow, L.; Mosbach, K. *FEBS Lett.* **1987**, *210*, 147–152.
- Tokumura, A. *J. Cell. Biochem.* **2004**, *92*, 869–881.
- Tang, S.-P.; Hu, P.; Chen, H.-Y.; Chen, S.; Mao, Z.-W.; Ji, L.-N. *J. Mol. Cat. A: Chem.* **2011**, *335*, 222–227.
- Fragoso, A.; Baratto, M. C.; Diaz, A.; Rodriguez, Y.; Pogni, R.; Basosi, R.; Cao, R. *Dalton Trans.* **2004**, 1456–1460.
- Yan, J.; Breslow, R. *Tetrahedron Lett.* **2000**, *41*, 2059–2062.
- Nelson, D. R. *Arch. Biochem. Biophys.* **1999**, *369*, 1–10.
- Danielson, P. B. *Curr. Drug Metab.* **2002**, *3*, 561–597.
- Cai, Y.; Liu, Y.; Lu, Y.; Gao, G.; He, M. *Catal. Lett.* **2008**, *124*, 334–339.
- Schening, A. P. H. J.; Spelberg, J. H. L.; Hubert, D. H. W.; Feiters, M. C.; Molte, R. J. M. *Chem.—Eur. J.* **1998**, *4*, 871–880.
- Hessenauer-Ilicheva, N.; Franke, A.; Meyer, D.; Woggon, W.-D.; van Eldik, R. *J. Am. Chem. Soc.* **2007**, *129*, 12473–12479.
- Schlichting, I.; Berendzen, J.; Chu, K.; Stock, A. M.; Maves, S. A.; Benson, D. E.; Sweet, R. M.; Ringe, D.; Petsko, G. A.; Sligar, S. G. *Science* **2000**, *287*, 1615–1622.
- Cho, S. Y.; Kim, J.-H.; Paik, Y.-K. *Mol. Cell* **1998**, *8*, 233–239.
- Fang, Z.; Breslow, R. *Bioorg. Med. Chem. Lett.* **2005**, *15*, 5463–5466.
- Breslow, R.; Yan, J.; Belvedere, S. *Tetrahedron Lett.* **2002**, *43*, 363–365.

- (74) Breslow, R.; Yang, J.; Yan, J. *Tetrahedron* **2002**, *58*, 653–659.
- (75) Kanagaraj, K.; Suresh, P.; Pitchumani, K. *Org. Lett.* **2010**, *12*, 4070–4073.
- (76) Breslow, R.; Czarnik, A. W.; Lauer, M.; Leppkes, R.; Winkler, J.; Zimmerman, S. *J. Am. Chem. Soc.* **1986**, *108*, 1969–1979.
- (77) Breslow, R.; Chmielewski, J.; Foley, D.; Johnson, B.; Kumabe, N.; Varney, M.; Mehra, R. *Tetrahedron* **1988**, *44*, 5515–5524.
- (78) Tabushi, I.; Kuroda, Y.; Yamada, M.; Higashimura, H.; Breslow, R. *J. Am. Chem. Soc.* **1985**, *107*, 5545–5546.
- (79) Fasella, E.; Dong, S. D.; Breslow, R. *Bioorg. Med. Chem.* **1999**, *7*, 709–714.
- (80) Freeman, W. A.; Mock, W. L.; Shih, N. Y. *J. Am. Chem. Soc.* **1981**, *103*, 7367–7368.
- (81) Kim, J.; Jung, I.-S.; Kim, S.-Y.; Lee, E.; Kang, J.-K.; Sakamoto, S.; Yamaguchi, K.; Kim, K. *J. Am. Chem. Soc.* **2000**, *122*, 540–541.
- (82) Day, A.; Arnold, A. P.; Blanch, R. J.; Snushall, B. *J. Org. Chem.* **2001**, *66*, 8094–8100.
- (83) Buschmann, H.-J.; Jansen, K.; Schollmeyer, E. *Thermochim. Acta* **1998**, *317*, 95–98.
- (84) Buschmann, H.-J.; Cleve, E.; Schollmeyer, E. *Inorg. Chim. Acta* **1992**, *193*, 93–97.
- (85) Mock, W. L.; Shih, N. Y. *J. Am. Chem. Soc.* **1989**, *111*, 2697–2699.
- (86) Mock, W. L.; Shih, N. Y. *J. Org. Chem.* **1983**, *48*, 3618–3619.
- (87) Hennig, A.; Bakirci, H.; Nau, W. M. *Nat. Methods* **2007**, *4*, 629–632.
- (88) Klock, C.; Souza, R. N.; Nau, W. M. *Org. Lett.* **2009**, *11*, 2595–2598.
- (89) Liu, S.; Ruspic, C.; Mukhopadhyay, P.; Chakrabarti, S.; Zavalij, P. Y.; Isaacs, L. *J. Am. Chem. Soc.* **2005**, *127*, 15959–15967.
- (90) Chakrabarti, S.; Mukhopadhyay, P.; Lin, S.; Isaacs, L. *Org. Lett.* **2007**, *9*, 2349–2352.
- (91) Day, A. I.; Blanch, R. J.; Arnold, A. P.; Lorenzo, S.; Lewis, G. R.; Dance, I. *Angew. Chem., Int. Ed.* **2002**, *41*, 275–277.
- (92) Pattabiraman, M.; Natarajan, A.; Kaanumalle, L. S.; Ramamurthy, V. *Org. Lett.* **2005**, *7*, 529–532.
- (93) Mock, W. L.; Shih, N. Y. *J. Org. Chem.* **1986**, *51*, 4440–4446.
- (94) Ghosh, S.; Isaacs, L. *J. Am. Chem. Soc.* **2010**, *132*, 4445–4454.
- (95) Dumoulin, M.; Kumita, J. R.; Dobson, C. M. *Acc. Chem. Res.* **2006**, *39*, 603–610.
- (96) Lindsey, J. S. *New J. Chem.* **1991**, *15*, 153–180.
- (97) Whitesides, G. M.; Grzybowski, B. *Science* **2002**, *295*, 2418–2421.
- (98) Newcomer, M. E.; Gilbert, N. C. *J. Biol. Chem.* **2010**, *285*, 25109–25114.
- (99) Biradha, K.; Fujita, M. *Adv. Supramol. Chem.* **2000**, *6*, 1–39.
- (100) Northrop, B. H.; Zheng, Y.-R.; Chi, K.-W.; Stang, P. J. *Acc. Chem. Res.* **2009**, *42*, 1554–1563.
- (101) Fiedler, D.; Leung, D. H.; Bergman, R. G.; Raymond, K. N. *Acc. Chem. Res.* **2005**, *38*, 349–358.
- (102) Fujita, M.; Tominaga, M.; Hori, A.; Therrien, B. *Acc. Chem. Res.* **2005**, *38*, 369–378.
- (103) Fujita, M.; Yazaki, J.; Ogura, K. *J. Am. Chem. Soc.* **1990**, *112*, 5645–5647.
- (104) Fujita, M.; Nagao, S.; Iida, M.; Ogata, K.; Ogura, K. *J. Am. Chem. Soc.* **1993**, *115*, 1574–1576.
- (105) Stang, P. J. *J. Org. Chem.* **2009**, *74*, 2–20.
- (106) Stang, P. J.; Cao, D. H. *J. Am. Chem. Soc.* **1994**, *116*, 4981–4982.
- (107) Stang, P. J.; Whiteford, J. A. *Organometallics* **1994**, *13*, 3776–3777.
- (108) Stang, P. J.; Chen, K. *J. Am. Chem. Soc.* **1995**, *117*, 1667–1668.
- (109) Stang, P. J.; Persky, N. E. *Chem. Commun.* **1997**, 77–78.
- (110) Fujita, M.; Oguro, D.; Miyazawa, M.; Oka, H.; Yamaguchi, K.; Ogura, K. *Nature* **1995**, *378*, 469–471.
- (111) Fujita, M.; Nagao, S.; Ogura, K. *J. Am. Chem. Soc.* **1995**, *117*, 1649–1650.
- (112) Yoshizawa, M.; Tamura, M.; Fujita, M. *Science* **2006**, *312*, 251–254.
- (113) Nishioka, Y.; Yamaguchi, T.; Kawano, M.; Fujita, M. *J. Am. Chem. Soc.* **2008**, *130*, 8160–8161.
- (114) Murase, T.; Horiuchi, S.; Fujita, M. *J. Am. Chem. Soc.* **2010**, *132*, 2866–2867.
- (115) Nishioka, Y.; Yamaguchi, T.; Yoshizawa, M.; Fujita, M. *J. Am. Chem. Soc.* **2007**, *129*, 7000–7001.
- (116) Yoshizawa, M.; Takeyama, Y.; Okano, T.; Fujita, M. *J. Am. Chem. Soc.* **2003**, *125*, 3243–3247.
- (117) Yoshizawa, M.; Takeyama, Y.; Kusukawa, T.; Fujita, M. *Angew. Chem., Int. Ed.* **2002**, *41*, 1347–1349.
- (118) Beissel, T.; Powers, R. E.; Raymond, K. N. *Angew. Chem., Int. Ed.* **1996**, *35*, 1084–1086.
- (119) Brown, C. J.; Bergman, R. G.; Raymond, K. N. *J. Am. Chem. Soc.* **2009**, *131*, 17530–17531.
- (120) Davis, A. V.; Fiedler, D.; Ziegler, M.; Terpin, A.; Raymond, K. N. *J. Am. Chem. Soc.* **2007**, *129*, 15354–15363.
- (121) Fiedler, D.; Bergman, R. G.; Raymond, K. N. *Angew. Chem., Int. Ed.* **2006**, *45*, 745–748.
- (122) Brumaghim, J. L.; Michels, M.; Pagliero, D.; Raymond, K. N. *Eur. J. Org. Chem.* **2004**, 5115–5118.
- (123) Hastings, C. J.; Pluth, M. D.; Bergman, R. G.; Raymond, K. N. *J. Am. Chem. Soc.* **2010**, *132*, 6938–6940.
- (124) Pluth, M. D.; Bergman, R. G.; Raymond, K. N. *Science* **2007**, *316*, 85–88.
- (125) Pluth, M. D.; Bergman, R. G.; Raymond, K. N. *Angew. Chem., Int. Ed.* **2007**, *46*, 8587–8589.
- (126) Hastings, C. J.; Fiedler, D.; Bergman, R. G.; Raymond, K. N. *J. Am. Chem. Soc.* **2008**, *130*, 10977–10983.
- (127) Purse, B. W.; Rebek, J., Jr. *Proc. Natl. Acad. Sci. U.S.A.* **2005**, *102*, 10777–10782.
- (128) Hoegberg, A. G. S. *J. Am. Chem. Soc.* **1980**, *102*, 6046–6050.
- (129) Hoegberg, A. G. S. *J. Org. Chem.* **1980**, *45*, 4498–4500.
- (130) Rudkevich, D. M.; Hilmersson, G.; Rebek, J., Jr. *J. Am. Chem. Soc.* **1997**, *119*, 9911–9912.
- (131) Far, A. R.; Shivanyuk, A.; Rebek, J., Jr. *J. Am. Chem. Soc.* **2002**, *124*, 2854–2855.
- (132) Hof, F.; Trembleau, L.; Ullrich, E. C.; Rebek, J., Jr. *Angew. Chem., Int. Ed.* **2003**, *42*, 3150–3153.
- (133) Starnes, S. D.; Rudkevich, D. M.; Rebek, J., Jr. *Org. Lett.* **2000**, *2*, 1995–1998.
- (134) Luecking, U.; Chen, J.; Rudkevich, D. M.; Rebek, J., Jr. *J. Am. Chem. Soc.* **2001**, *123*, 9929–9934.
- (135) Richeter, S.; Rebek, J., Jr. *J. Am. Chem. Soc.* **2004**, *126*, 16280–16281.
- (136) Hooley, R. J.; Rebek, J., Jr. *Org. Biomol. Chem.* **2007**, *5*, 3631–3636.
- (137) Chen, J.; Rebek, J., Jr. *Org. Lett.* **2002**, *4*, 327–329.
- (138) Butterfield, S. M.; Rebek, J., Jr. *Chem. Commun.* **2007**, 1605–1607.
- (139) Lee, H.; Son, S. H.; Sharma, R.; Won, Y.-Y. *J. Phys. Chem. B* **2011**, *115*, 844–860.
- (140) Suh, J.; Klotz, I. M. *J. Am. Chem. Soc.* **1984**, *106*, 2373–2378.
- (141) Arcelli, A.; Concilio, C. *J. Org. Chem.* **1996**, *61*, 1682–1688.
- (142) Koplín, S. A.; Lin, S.; Domanski, T. *Biotechnol. Prog.* **2008**, *24*, 1160–1165.
- (143) Zhao, H.; Breslow, R. *Bioorg. Med. Chem. Lett.* **2010**, *20*, 5973–5975.
- (144) Yudovin-Farber, I.; Golenser, J.; Beyth, N.; Weiss, E. I.; Domb, A. J. *J. Nanomaterials* **2010**, 1–11.
- (145) Rosenholm, J. M.; Duchanoy, A.; Linden, M. *Chem. Mater.* **2008**, *20*, 1126–1133.
- (146) Poe, S. L.; Kobaslija, M.; McQuade, D. T. *J. Am. Chem. Soc.* **2007**, *129*, 9216–9221.
- (147) Klotz, I. M.; Royer, G. P.; Scarpa, I. S. *Proc. Natl. Acad. Sci. U.S.A.* **1971**, *68*, 263–264.
- (148) Kiefer, H. C.; Congdon, W. I.; Scarpa, I. S.; Klotz, I. M. *Proc. Natl. Acad. Sci. U.S.A.* **1972**, *69*, 2155–2159.

- (149) Zhou, W.; Liu, L.; Breslow, R. *Helv. Chim. Acta* **2003**, *86*, 3560–3567.
- (150) Liu, L.; Rozenman, M.; Breslow, R. *J. Am. Chem. Soc.* **2002**, *124*, 12660–12661.
- (151) Liu, L.; Breslow, R. *J. Am. Chem. Soc.* **2002**, *124*, 4978–4979.
- (152) Saegusa, T.; Ikeda, H.; Fujii, H. *Macromolecules* **1972**, *5*, 108.
- (153) Saegusa, T.; Ikeda, H.; Fujii, H. *Polym. J.* **1972**, *3*, 35–39.
- (154) Kobayashi, S.; Iijima, S.; Igarashi, T.; Saegusa, T. *Macromolecules* **1987**, *20*, 1729–1734.
- (155) Bandyopadhyay, S.; Zhou, W.; Breslow, R. *Org. Lett.* **2007**, *9*, 1009–1012.
- (156) Levine, M.; Kenesky, C. S.; Zheng, S.; Quinn, J.; Breslow, R. *Tetrahedron Lett.* **2008**, *49*, 5746–5750.
- (157) Zhou, W.; Yerkes, N.; Chruma, J. J.; Liu, L.; Breslow, R. *Bioorg. Med. Chem. Lett.* **2005**, *15*, 1351–1355.
- (158) Liu, L.; Etika, K. C.; Liao, K.-S.; Hess, L. A.; Bergbreiter, D. E.; Grunlan, J. C. *Macromol. Rapid Commun.* **2009**, *30*, 627–632.
- (159) Hashemi, M.; Parhiz, B. H.; Hatefi, A.; Ramezani, M. *Cancer Gene Ther.* **2011**, *18*, 12–19.
- (160) Peng, Q.; Chen, F.; Zhong, Z.; Zhuo, R. *Chem. Commun.* **2010**, *46*, 5888–5890.
- (161) Schaefer, J.; Hoebel, S.; Bakowsky, U.; Aigner, A. *Biomaterials* **2010**, *31*, 6892–6900.
- (162) Zhao, H.; Foss, F. W.; Breslow, R. *J. Am. Chem. Soc.* **2008**, *130*, 12590–12591.
- (163) Breslow, R. *J. Am. Chem. Soc.* **1957**, *79*, 1762–1763.
- (164) Price, K. E.; Broadwater, S. J.; Bogdan, A. R.; Keresztes, I.; Steinbacher, J. L.; McQuade, D. T. *Macromolecules* **2006**, *39*, 7681–7685.
- (165) Poe, S. L.; Kobaslija, M.; McQuade, D. T. *J. Am. Chem. Soc.* **2006**, *128*, 15586–15587.
- (166) Evans, D. A.; Seidel, D. J. *J. Am. Chem. Soc.* **2005**, *127*, 9958–9959.
- (167) Chi, Y.; Scroggins, S. T.; Boz, E.; Frechet, J. M. J. *J. Am. Chem. Soc.* **2008**, *130*, 17287–17289.
- (168) Mukherjee, S.; Yang, J. W.; Hoffmann, S.; List, B. *Chem. Rev.* **2007**, *107*, 5471–5569.
- (169) Wulff, G. *Chem. Rev.* **2002**, *102*, 1–27.
- (170) Haupt, K.; Mosbach, K. *Chem. Rev.* **2000**, *100*, 2495–2504.
- (171) Bugg, T. D. H. *Wiley Encyclopedia of Chemical Biology*; John Wiley & Sons: Hoboken, NJ, 2009; Vol. 1; pp 653–663.
- (172) Ye, L.; Mosbach, K. *Chem. Mater.* **2008**, *20*, 859–868.
- (173) Wulff, G.; Vesper, W.; Grobe-Einsler, R.; Sarhan, A. *Makromol. Chem.* **1977**, *178*, 2799–2816.
- (174) Wulff, G.; Grobe-Einsler, R.; Vesper, W.; Sarhan, A. *Makromol. Chem.* **1977**, *178*, 2817–2825.
- (175) Sellergren, B.; Karmalkar, R. N.; Shea, K. J. *J. Org. Chem.* **2000**, *65*, 4009–4027.
- (176) Wulff, G.; Vietmeier, J. *Makromol. Chem.* **1989**, *190*, 1727–1735.
- (177) Andersson, L. I.; Mosbach, K. *Makromol. Chem. Rapid Commun.* **1989**, *10*, 491–495.
- (178) Wulff, G.; Schauhoff, S. J. *J. Org. Chem.* **1991**, *56*, 395–400.
- (179) Xu, Z.; Kuang, D.; Feng, Y.; Zhang, F. *Carbohydr. Polym.* **2010**, *79*, 642–647.
- (180) Yu, C.; Mosbach, K. *J. Org. Chem.* **1997**, *62*, 4057–4064.
- (181) Chen, W.; Han, D.-K.; Ahn, K.-D.; Kim, J.-M. *Macromol. Res.* **2002**, *10*, 122–126.
- (182) Nopper, D.; Lammershop, O.; Wulff, G.; Gauglitz, G. *Anal. Bioanal. Chem.* **2003**, *377*, 608–613.
- (183) Strikovskiy, A. G.; Kasper, D.; Gruen, M.; Green, B. S.; Hradil, J.; Wulff, G. *J. Am. Chem. Soc.* **2000**, *122*, 6295–6296.
- (184) Emgenbroich, M.; Wulff, G. *Chem.—Eur. J.* **2003**, *9*, 4106–4117.
- (185) Svenson, J.; Zheng, N.; Nicholls, I. A. *J. Am. Chem. Soc.* **2004**, *126*, 8554–8560.
- (186) Karlsson, J. G.; Andersson, L. I.; Nicholls, I. A. *Anal. Chim. Acta* **2001**, *435*, 57–64.
- (187) Carboni, D.; Flavin, K.; Servant, A.; Gouverneur, V.; Resmini, M. *Chem.—Eur. J.* **2008**, *14*, 7059–7065.
- (188) Liu, J.-Q.; Wulff, G. *Angew. Chem., Int. Ed.* **2004**, *43*, 1287–1290.
- (189) Hedin-Dahlstrom, J.; Rosengren-Holmberg, J. P.; Legrand, S.; Wikman, S.; Nicholls, I. A. *J. Org. Chem.* **2006**, *71*, 4845–4853.
- (190) Matsui, J.; Nicholls, I. A.; Karube, I.; Mosbach, K. *J. Org. Chem.* **1996**, *61*, 5414–5417.
- (191) Liu, X. C.; Mosbach, K. *Macromol. Rapid Commun.* **1997**, *18*, 609–615.
- (192) Zhang, H.; Piacham, T.; Drew, M.; Patek, M.; Mosbach, K.; Ye, L. *J. Am. Chem. Soc.* **2006**, *128*, 4178–4179.
- (193) Zimmerman, S. C.; Zharov, I.; Wendland, M. S.; Rakow, N. A.; Suslick, K. S. *J. Am. Chem. Soc.* **2003**, *125*, 13504–13518.
- (194) MacMillan, D. W. C. *Nature* **2008**, *455*, 304–308.
- (195) Jacobsen, E. N.; MacMillan, D. W. C. *Proc. Natl. Acad. Sci. U.S.A.* **2010**, *107*, 20618–20619.
- (196) Enders, D.; Narine, A. A. *J. Org. Chem.* **2008**, *73*, 7857–7870.
- (197) Davie, E. A. C.; Mennen, S. M.; Xu, Y.; Miller, S. J. *Chem. Rev.* **2007**, *107*, 5759–5812.
- (198) Knowles, R. R.; Jacobsen, E. N. *Proc. Natl. Acad. Sci. U.S.A.* **2010**, *107*, 20678–20685.
- (199) List, B. *Chem. Commun.* **2006**, 819–824.
- (200) Lelais, G.; MacMillan, D. W. C. *Aldrichim. Acta* **2006**, *39*, 79–87.
- (201) Enders, D.; Grondal, C.; Huettl, M. R. M. *Angew. Chem., Int. Ed.* **2007**, *46*, 1570–1581.
- (202) Miller, S. J. *Acc. Chem. Res.* **2004**, *37*, 601–610.
- (203) Lewis, C. A.; Gustafson, J. L.; Chiu, A.; Balsells, J.; Pollard, D.; Murry, J.; Reamer, R. A.; Hansen, K. B.; Miller, S. J. *J. Am. Chem. Soc.* **2008**, *130*, 16358–16365.
- (204) Lewis, C. A.; Chiu, A.; Kubryk, M.; Balsells, J.; Pollard, D.; Esser, C. K.; Murry, J.; Reamer, R. A.; Hansen, K. B.; Miller, S. J. *J. Am. Chem. Soc.* **2006**, *128*, 16454–16455.
- (205) Sculimbrene, B. R.; Miller, S. J. *J. Am. Chem. Soc.* **2001**, *123*, 10125–10126.
- (206) Guerin, D. J.; Horstmann, T. E.; Miller, S. J. *Org. Lett.* **1999**, *1*, 1107–1109.
- (207) Gustafson, J. L.; Lim, D.; Miller, S. J. *Science* **2010**, *328*, 1251–1255.
- (208) Uyeda, C.; Roetheli, A. R.; Jacobsen, E. N. *Angew. Chem., Int. Ed.* **2010**, *49*, 9753–9756.
- (209) Uyeda, C.; Jacobsen, E. N. *J. Am. Chem. Soc.* **2008**, *130*, 9228–9229.
- (210) Knowles, R. R.; Lin, S.; Jacobsen, E. N. *J. Am. Chem. Soc.* **2010**, *132*, 5030–5032.
- (211) Barbas, C. F., III. *Angew. Chem., Int. Ed.* **2008**, *47*, 42–47.
- (212) Hajos, Z. G.; Parrish, D. R. *J. Org. Chem.* **1974**, *39*, 1615–1621.
- (213) Eder, U.; Sauer, G.; Wiechert, R. *Angew. Chem., Int. Ed.* **1971**, *10*, 496–497.
- (214) Gefflaut, T.; Blonski, C.; Perie, J.; Willson, M. *Prog. Biophys. Mol. Biol.* **1995**, *63*, 301–340.
- (215) Rutter, W. J. *Fed. Proc.* **1964**, *23*, 1248–1257.
- (216) Lerner, R. A.; Barbas, C. F., III. *Acta Chem. Scand.* **1996**, *50*, 672–678.
- (217) Allemann, C.; Gordillo, R.; Clemente, F. R.; Cheong, P. H. Y.; Houk, K. N. *Acc. Chem. Res.* **2004**, *37*, 558–569.
- (218) Zhu, H.; Clemente, F. R.; Houk, K. N.; Meyer, M. P. *J. Am. Chem. Soc.* **2009**, *131*, 1632–1633.
- (219) Hoang, L.; Bahmanyar, S.; Houk, K. N.; List, B. *J. Am. Chem. Soc.* **2003**, *125*, 16–17.
- (220) Ahrendt, K. A.; Borths, C. J.; MacMillan, D. W. C. *J. Am. Chem. Soc.* **2000**, *122*, 4243–4244.
- (221) Jung, M. E.; Vaccaro, W. D.; Buszek, K. R. *Tetrahedron Lett.* **1989**, *30*, 1893–1896.
- (222) List, B.; Lerner, R. A.; Barbas, C. F., III. *J. Am. Chem. Soc.* **2000**, *122*, 2395–2396.
- (223) Austin, J. F.; MacMillan, D. W. C. *J. Am. Chem. Soc.* **2002**, *124*, 1172–1173.
- (224) Chen, Y. K.; Yoshida, M.; MacMillan, D. W. C. *J. Am. Chem. Soc.* **2006**, *128*, 9328–9329.

- (225) Brown, S. P.; Goodwin, N. C.; MacMillan, D. W. C. *J. Am. Chem. Soc.* **2003**, *125*, 1192–1194.
- (226) Mangion, I. K.; Northrup, A. B.; MacMillan, D. W. C. *Angew. Chem., Int. Ed.* **2004**, *43*, 6722–6724.
- (227) List, B. *Tetrahedron* **2002**, *58*, 5573–5590.
- (228) Mase, N.; Nakai, Y.; Ohara, N.; Yoda, H.; Takabe, K.; Tanaka, F.; Barbas, C. F., III. *J. Am. Chem. Soc.* **2006**, *128*, 734–735.
- (229) Fessner, W.-D.; Jennewein, S. *Biocatalysis in the Pharmaceutical and Biotechnology Industries*; CRC Press: Boca Raton, FL, 2007, pp 363–400.
- (230) Barbas, C. F., III.; Wang, Y. F.; Wong, C. H. *J. Am. Chem. Soc.* **1990**, *112*, 2013–2014.
- (231) Thayumanavan, R.; Tanaka, F.; Barbas, C. F., III. *Org. Lett.* **2004**, *6*, 3541–3544.
- (232) Baer, K.; Dueckers, N.; Hummel, W.; Groeger, H. *Chem-CatChem* **2010**, *2*, 939–942.
- (233) Suri, J. T.; Mitsumori, S.; Albertshofer, K.; Tanaka, F.; Barbas, C. F., III. *J. Org. Chem.* **2006**, *71*, 3822–3828.
- (234) Hecquet, L.; Helaine, V.; Charmantray, F.; Lemaire, M. *Mod. Biocatal.* **2009**, 287–298.
- (235) Chowdari, N. S.; Ramachary, D. B.; Cordova, A.; Barbas, C. F., III. *Tetrahedron Lett.* **2002**, *43*, 9591–9595.
- (236) Yang, H.; Carter, R. G. *Synlett* **2010**, 2827–2838.
- (237) Guillena, G.; Najera, C.; Ramon, D. J. *Tetrahedron: Asymmetry* **2007**, *18*, 2249–2293.
- (238) Cordova, A.; Notz, W.; Zhong, G.; Betancort, J. M.; Barbas, C. F., III. *J. Am. Chem. Soc.* **2002**, *124*, 1842–1843.
- (239) List, B. *J. Am. Chem. Soc.* **2000**, *122*, 9336–9337.
- (240) List, B.; Pojarliev, P.; Biller, W. T.; Martin, H. J. *J. Am. Chem. Soc.* **2002**, *124*, 827–833.
- (241) Chowdari, N. S.; Suri, J. T.; Barbas, C. F., III. *Org. Lett.* **2004**, *6*, 2507–2510.
- (242) Nielsen, M.; Jacobsen, C. B.; Paixao, M. W.; Holub, N.; Jorgensen, K. A. *J. Am. Chem. Soc.* **2009**, *131*, 10581–10586.
- (243) Zhong, G. *Angew. Chem., Int. Ed.* **2003**, *42*, 4247–4250.
- (244) Brown, S. P.; Brochu, M. P.; Sinz, C. J.; MacMillan, D. W. C. *J. Am. Chem. Soc.* **2003**, *125*, 10808–10809.
- (245) Bogeveg, A.; Sunden, H.; Cordova, A. *Angew. Chem., Int. Ed.* **2004**, *43*, 1109–1112.
- (246) Hayashi, Y.; Yamaguchi, J.; Sumiya, T.; Shoji, M. *Angew. Chem., Int. Ed.* **2004**, *43*, 1112–1115.
- (247) Mathew, S. P.; Iwamura, H.; Blackmond, D. G. *Angew. Chem., Int. Ed.* **2004**, *43*, 3317–3321.
- (248) Soai, K.; Shibata, T.; Morioka, H.; Choji, K. *Nature* **1995**, *378*, 767–768.
- (249) Puchot, C.; Samuel, O.; Dunach, E.; Zhao, S.; Agami, C.; Kagan, H. B. *J. Am. Chem. Soc.* **1986**, *108*, 2353–2357.
- (250) Kitamura, M.; Suga, S.; Oka, H.; Noyori, R. *J. Am. Chem. Soc.* **1998**, *120*, 9800–9809.
- (251) Blackmond, D. G.; McMillan, C. R.; Ramdeehul, S.; Schorm, A.; Brown, J. M. *J. Am. Chem. Soc.* **2001**, *123*, 10103–10104.
- (252) Kawasaki, T.; Soai, K. *J. Fluorine Chem.* **2010**, *131*, 525–534.
- (253) Breslow, R.; Levine, M. S. *Proc. Natl. Acad. Sci. U.S.A.* **2006**, *103*, 12979–12980.
- (254) Klussmann, M.; Iwamura, H.; Mathew, S. P.; Wells, D. H., Jr.; Pandya, U.; Armstrong, A.; Blackmond, D. G. *Nature* **2006**, *441*, 621–623.
- (255) Duggleby, R. G. *Acc. Chem. Res.* **2006**, *39*, 550–557.
- (256) Enders, D.; Breuer, K.; Raabe, G.; Runsink, J.; Teles, J. H.; Melder, J.-P.; Ebel, K.; Brode, S. *Angew. Chem., Int. Ed.* **1995**, *34*, 1021–1023.
- (257) Teles, J. H.; Melder, J. P.; Ebel, K.; Schneider, R.; Gehrler, E.; Harder, W.; Brode, S.; Enders, D.; Breuer, K.; Raabe, G. *Helv. Chim. Acta* **1996**, *79*, 61–83.
- (258) Enders, D.; Breuer, K.; Teles, J. H. *Helv. Chim. Acta* **1996**, *79*, 1217–1221.
- (259) Enders, D.; Kallfass, U. *Angew. Chem., Int. Ed.* **2002**, *41*, 1743–1745.
- (260) Enders, D.; Niemeier, O. *Synlett* **2004**, 2111–2114.
- (261) Kerr, M. S.; Read de Alaniz, J.; Rovis, T. *J. Org. Chem.* **2005**, *70*, 5725–5728.
- (262) Enders, D.; Breuer, K.; Runsink, J.; Teles, J. H. *Helv. Chim. Acta* **1996**, *79*, 1899–1902.
- (263) Jousseume, T.; Wurz, N. E.; Glorius, F. *Angew. Chem., Int. Ed.* **2011**, *50*, 1410–1414.
- (264) Liu, Q.; Rovis, T. *Org. Lett.* **2009**, *11*, 2856–2859.
- (265) Kim, S. M.; Jin, M. Y.; Kim, M. J.; Cui, Y.; Kim, Y. S.; Zhang, L.; Song, C. E.; Ryu, D. H.; Yang, J. W. *Org. Biomol. Chem.* **2011**, *9*, 2069–2071.
- (266) Read de Alaniz, J.; Kerr, M. S.; Moore, J. L.; Rovis, T. *J. Org. Chem.* **2008**, *73*, 2033–2040.
- (267) Hawkes, K. J.; Yates, B. F. *Eur. J. Org. Chem.* **2008**, 5563–5570.
- (268) Grondal, C.; Jeanty, M.; Enders, D. *Nat. Chem.* **2010**, *2*, 167–178.
- (269) Westermann, B.; Ayaz, M.; van Berkel, S. S. *Angew. Chem., Int. Ed.* **2010**, *49*, 846–849.
- (270) Alba, A.-N.; Companyo, X.; Viciano, M.; Rios, R. *Curr. Org. Chem.* **2009**, *13*, 1432–1474.
- (271) Schetter, B.; Mahrwald, R. *Angew. Chem., Int. Ed.* **2006**, *45*, 7506–7525.
- (272) Dondoni, A.; Massi, A. *Angew. Chem., Int. Ed.* **2008**, *47*, 4638–4660.